Development of a novel extraction method for the analysis of prostaglandins and leukotrienes in fish liver by using liquid chromatography mass spectrometry

By

Joseph Diab

Thesis for the degree of European Master in Quality in Analytical Laboratories

Bergen, Norway
August 2015

Department of Chemistry
University of Bergen
Bergen, Norway

National Institute of nutrition
and seafood research
Bergen, Norway

Development of a novel extraction method for the analysis of prostaglandins and leukotrienes in fish liver by using liquid chromatography mass spectrometry

By

Joseph Diab

Thesis for the degree of European Master in Quality in Analytical Laboratories

Supervisors
Pedro Araujo, PhD
Professor, National Institute of Nutrition and Seafood Research

Bjørn Grung, PhD
Professor, Department of Chemistry, University of Bergen

Bergen, Norway
August 2015

Contents

Acknowledgments

This work was carried out at the National Institute of Nutrition and Seafood Research (NIFES) in Bergen under the supervision of Prof. Pedro Araujo and Prof. Bjørn Grung. The work was supported by Erasmus Mundus Master in Quality in Analytical Laboratories (EMQAL).

I would like to first express my sincere gratitude to Prof. Pedro Araujo for his patience during my work, I have learned a lot from his advises and knowledge on both professional and personal level, I was honored to be a student under the supervision of such scientist.

I would not be able to complete this work without the support of Prof. Bjørn Grung and his motivation since the first time I met him in Barcelona, thanks for introducing me in the amazing world of data analysis and chemometrics.

Dr Nini Seesener is also acknowledged for supplying fish samples and giving me a lot of help in fish biology and nutrition.

I feel very grateful to Prof. Angeles Sahouqillo and Prof. Miguel Esteban from University Barcelona, Spain, without their direction, EMQAL 2014-15 would never exist, thank you for giving my colleagues and me the chance to enroll in this master and such a career opportunity.

My family and friends in Syria, you never stopped encouraging me during my study, I will keep carrying you in my heart whenever I go.

Last but not least, thanks all the personnel in NIFES for their technical assistance, especially Bashir who always treated me like a young brother.

Thanks to my colleagues from EMQAL: Moises, Karen, Marta, Tom, Tea and Jovana, I wish each one of you the very best in life, I was also privileged to meet true friends during my exchange student life in Norway, Betty, Chloe, Aude, Sabrina, and Nathalie every moment I shared with you will always be remembered.

Finally, every tragedy must come to an end and the war shall over, a time will come when I will take part serving my beloved country, and help building the future Syria, until then, may God protect all the Syrians around the world, we shall go back … one day….

List of Abbreviation

Polyunsaturated fatty acids	PUFAs
Linoleic acid	LA
α-Linolenic acid	α-LNA/ALA
Arachidonic acid	AA
Eicosapentaenoic acid	EPA
Docosahexaenoic acid	DHA
Cyclooxygenases	COX
Stearidonic acid	SDA
Eicosatetraoisic	ETA
Lipooxygenases	LOX
Enzyme immunoassay	EIA
Radioimmunoassay	RIA
Gas chromatography	GC
Liquid Chromatography	LC
High performance liquid chromatography	HPLC
Ultra performance liquid chromatography	UPLC
Mass spectrometry	MS
Electro spray ionization	ESI
Solid phase extraction	SPE
Liquid extraction	LE
Total ion chromatogram	TIC
Extracted jon chromatogram	EIC
Response factor	RF
Limit of detection	LOD
Limit of quantification	LOQ
Standard deviation	SD
Relative Standard deviation	RSD
Coefficient of variation	CV

Abstract

Eicosanoids are the major metabolites of fatty acids and they have pro-inflammatory anti-inflammatory proprieties, their role and production in solid biological tissue is important due to correlation with many kinds of diseases. A simple and rapid liquid extraction method for extracting prostaglandin E2 (PGE_2) and leukotriene B4 (LTB_4) from salmon liver and further determination by LC-MS/MS was developed and validated. The optimal combination of chloroform, acetonitrile and formic acid was investigated by simplex extraction design. The applied criteria for selecting the optimal mixture composition were the visual observation of clearness of supernatant after centrifugation, and the strength of signals represented by peak areas of extracted ion chromatogram (EIC).

Adding 500 µL of acetonitrile and 500 µL of chloroform subsequently to 0.3 g of pulverized liver sample was found the optimum extraction system. Formic acid dissolved the liver tissue and was ruled out.

The quantitative analysis was carried out using internal standards and the concentrations of internal standards are determined by a Doehlert design to keep the response factors constant in the analytical range. After the determination of the endogenous level of PGE_2 and LTB_4 in the working sample the method was submitted to validation. The proposed method exhibited good selectivity and linearity over the range (1-50) ng/g for both LTB_4 and PGE_2 respectively. In addition, the endogenous levels for PGE_2 (87 ng/g) and LTB_4 (101 ng/g) indicate that the system linearity could be extended until 137 ng/g and 151 ng/g respectively.

A full method validation has been performed, the considered validation parameters were: selectivity, limit of detection, limit of quantification, linearity, analytical range, precision recovery and stability. Also, since a blank sample was not available, the relative limit of quantification taking the endogenous level was considered. The method precision for LTB_4 quantification was found 19-20.6% and the recovery ranged between 98.4-104%, the relative limit of quantification was found 15.5%. Both PGE_2 and LTB_4 were found stable at -80C° in a solution of acetonitrile:chloroform (1:1) after 24 hours.

Suggestions for future working plan were given covering method development improvement.

1. Introduction

1.1. Background

1.1.1 Fatty Acids and Eicosanoids

The metabolism of essential long chain polyunsaturated fatty acids (PUFAs) generates lipid mediators which have numerous functions in the regulation of cell proliferation, tissue repair, coagulation and immunity, they also play an important role in the pathogenesis of various diseases [1]. The omega 3 (ω-3) and omega 6 (ω-6) fatty acids are two kinds of PUFAs that cannot be synthesized by mammals and consequently they must be obtained from the diet. Thus, the effect of different ω-3 and ω-6 fatty acids is becoming important [2].

It is important to explain the way of symbolic naming of PUFAs since it is the naming system commonly used in scientific literature.

The symbol name contains the number of carbon atoms, the number of double bounds and the position of the first double bound which is labeled as ω or n while the methyl group is numbered as carbon one. As an example, linoleic acid (LA) has 18 carbons, two double bonds. The first double bound is located between the 6th and 7th carbons from the methyl end, so it is designated as n-6 (or ω-6) fatty acid, and the symbol name is 18:2n-6 [1].

Linoleic and α-linolenic (α-LNA or ALA, 18:3n-3) acids are representative of ω-6 and ω-3 fatty acids respectively, and Eicosanoids are known to be their metabolites. First, AA amd ALA released from membrane phospholipids by the action of various phospholipases, before LA is converted into arachidonic acid (AA, 20:4n-6), while, ALA is converted into eicosapentaenoic acid (EPA, 20:5n-3) and docosahexaenoic acid (DHA, 22:6n-3) by enzyme mediated elongation and desaturation processes (Figure 1.1). The AA, as shown in Figure 1.2, is the substrate for two classes of enzymes, cyclooxygenases (COX), which produce 2-series prostaglandins, 2-series prostacyclin and 2-series thromboxane, and lipoxygenases (LOX), which catalyze the biosynthesis of hydroxyl eicosatetraenoic acids (HETEs) and 4-series leukotrienes, these are generally considered as pro-inflammatory eicosanoids. The EPA exhibits a similar metabolism to AA, but it is metabolized to 3-series prostaglandins, and thromboxane from COX and 5-series leukotrienes, hydroxyl eicosapentaenoic acids from LOX, and these are considered as anti-inflammatory eicosanoids [1].

The pro-inflammatory derived eicosanoids are positively linked to inflammatory diseases, such as arthritis and asthma, non-inflammatory diseases such as Alzheimer, cardiovascular diseases and cancer [3]. DHA are mainly converted to D-series resolvins by LOX. Resolvins is a new family of lipid mediators which possess both potent anti-inflammatory and immune-regulatory properties [1].

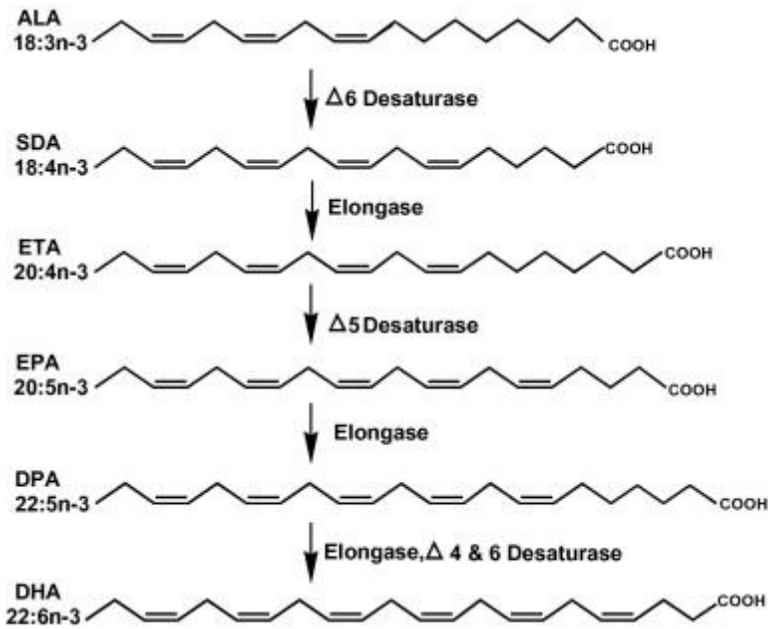

Figure 1.1 The formation of EPA and DHA from ALA [4].
SDA is stearidonic acid, ETA is Eicosatetraoisic acid

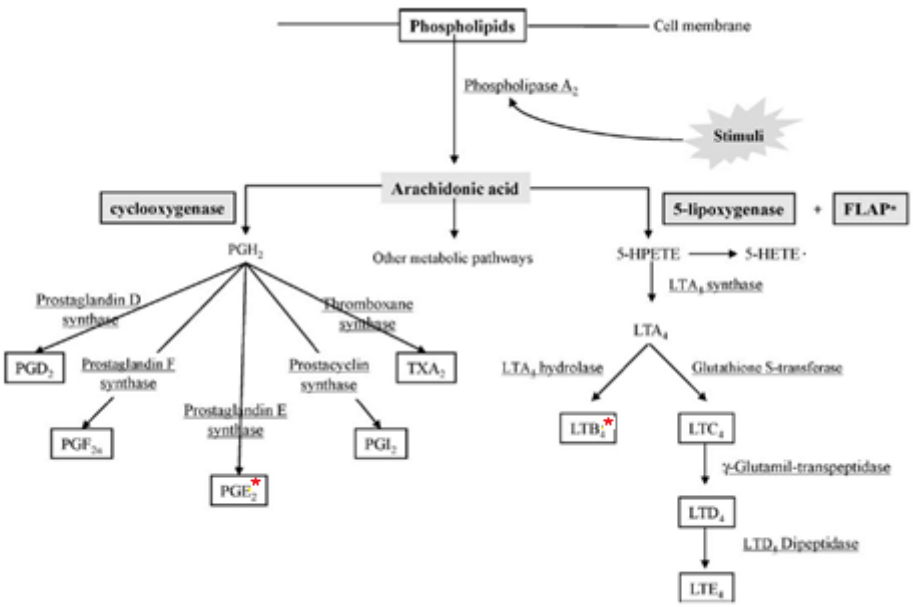

Fig. 1.2 Metabolism of arachidonic acid by the cyclooxygenase and 5-lipoxygenase pathways. (*) 5-Lipoxygenase-activating protein [4]. The eicosanoids of interest in this thesis are indicated by the red star.

1.1.2 Eicosanoids and the liver

Prostaglandins and leukotrienes were first isolated from the liver in 1970 [5]. Several in vivo and in vitro studies have demonstrated the cytoprotective effect of prostaglandins such as PGE_2 against viral induced hepatic injury. In addition, some researchers have indicated the role of some prostaglandins in the stimulation of blood flow in rat liver [5].

All liver cells produce eicosanoids (Table 1.1) but Kupffer cells and endothelial cells are quantitatively the most important. Kupffer cells produce both prostaglandin and leukotreins. The major prostaglandin are PGD_2, PGE_2, TxA_2, while the major leukotreins are LTB_4 and LTC_4. They play a role in protecting the organism from foreign and endogenous compounds. The anatomic location of the Kupffer cells lining the hepatic sinusoid allows filtering foreign particles, antigens, and endotoxins by releasing cytokine and generating inflammatory response while, at the same time, maintaining an appropriate inflammatory response and cytoprotective response by releasing PGE_2, which has a cytoprotective effect on the adjacent hepatocytes, and exerts a negative feedback on cytokine release [5].

Endothelial cells produce primarily PGI_2, which protects the liver by counteracting vasoconstriction, platelet aggregation, and leukocyte adherence. This protects the microcirculation of the liver during injury [5].

Unfortunately, the involvement of eicosanoids in fish liver functions have not been studied yet. Table 1.1 shows the production and action of different eicosanoid by different types of liver cells [5].

Table 1.1 The production and action of eicosanoids by different types of liver cells*

Cell source	Eicosanoids	Actions
Kupffer cells	PGD_2	Vasoconstriction
	PGE_2	$\downarrow IL_2$, $\downarrow LTB_4$, vasodilation, $\downarrow IL_1$ $\downarrow TNF\alpha$, cytoprotective to hepatocyte
	$PGF_{2\alpha}$	Vasoconstriction
	TxA_2	Vasoconstriction
	LTB_4	$\uparrow$ chemotaxis, $\uparrow$ vascular permeability, leukocyte adherence
	LTD_4	Shock
Endothelial cells	PGI_2	Vasodilation
	PGE_2	$\downarrow IL_1$, vasodilation $\downarrow IL_2$, $\downarrow LTB_4$, $\downarrow TNF_\alpha$
	$PGF_{2\alpha}$	Vasoconstriction
	LTE_4	
Hepatocytes	PGI_2	Small amounts, functional significance uncertain, hepatocytes mostly degrades eicosanoids
	PGE_2	
	$PGF_{2\alpha}$	
	TxA_2	
	LTB_4	
	EETs	

1.2 Eicosanoid analysis

1.2.1 Instrumental techniques

The main challenge of the analysis of PUFA metabolites in cells, tissues and body fluids are: the low endogenous concentrations (~pmol/mg to fmol/mg range), the multitude of isomeric and isobaric structures, and the risk of in vitro generation during sample pretreatment [6, 7].

Eicosanoids are generally analyzed by gas chromatography-mass spectrometry (GC–MS), liquid chromatography-mass spectrometry (LC-MS), enzyme immunoassay (EIA) and radioimmunoassay (RIA) as shown in Table 1.2. Although EIA is the most widely acknowledged methods for estimation of prostaglandins in biological samples, it has certain limitations due to its lack of specificity and its inability to determine multiple analytes in a single set of analyses. In addition, the levels of prostaglandins might be overestimated due to the possible cross reactivity of the antibody with different prostaglandins and the interference

of the fatty acid present in the sample matrix, resulting in a reduced selectivity, as well as the variability in the quantification of sequential samples [7, 8].

Table 1.2 Overview of the number of the application of different instrumental techniques for the analysis of eicosanoids in tissues in the last 30 years.

Tissue type	RIA	EIA	GCMS	LC	LCMS	UPLC
Brain	3 [10-12]	1 [11]	6 [13-18]	5 [14,19-23]	12 [22-34]	3 [35-37]
Lung	4 [38-41]	2 [39, 42, 43]	2 [39, 44]		5 [45-48]	
Kidney	2 [49, 50]		1 [52]		2 [51, 52]	
Muscle						1 [53]
Bone					1 [54]	
Skin	1 [55]	3 [56, 58]		1 [59]	1 [60]	
Liver	2 [61, 62]				4 [25, 33, 63, 64]	
Gonad			2 [65,66]		1 [67]	
Prostate				1 [68]	4 [8, 33, 48, 51]	
Breast	2 [43, 69]					
Colon	1 [70]	4 [71-75]			7 [63, 72, 76-80]	1 [81]

Corresponding references are given in square brackets

GC–MS provides greater sensitivity and selectivity for eicosanoid analysis, but requires chemical derivatization steps that limit its application since the analytical compounds must be both volatile and thermally stable in order to perform GC/MS based analyses.

The rapid progress of liquid-chromatography–electrospray ionization tandem mass spectrometry (LC–ESI-MS/MS) and the simplification of sample preparation have facilitated the use of this technology for accurate monitoring of eicosanoid metabolites in biological samples [7, 8]. In this technique, the LC component separates the eicosanoids based upon physical properties and it is followed by the MS component for identification based upon the characteristic product ions. Reversed phase chromatography is most commonly used because most eicosanoids, which are medium to nonpolar, elute in order of increasing hydrophobicity with a hydrophobic stationary phase (e.g., C18). The first step in mass spectrometry analysis is

to convert the analyte molecules into gas phase ions. Following ion production, the ions are separated by a mass analyzer that measures the mass to charge ratio (m/z) [6].

The main difference between analyzer are:

1. Their mass range limits (the upper limit of the mass of the ion that can be measured).
2. Acquisition rate (the rate at which the mass analyzer measures scans over a particular mass range).
3. Transmission range (the ratio of the number of ions reaching the detector to the number of ions leaving the source).
4. Mass accuracy (accuracy of the ion mass measurement provided by the mass analyzer).
5. Resolution (ability of a mass analyzer to yield 50% valley separation between distinct signals of two ions).

In ESI the ionization process occurs by applying a strong electric field, under atmospheric pressure, to a liquid passing through a capillary tube. This field induces a charge accumulation at the liquid surface located at the end of the capillary which causes droplets that contain an excess positive or negative charge to detach from the capillary tip and move toward the mass analyzer, then the solvent evaporates by an uncharged gas (e.g. nitrogen) forcing the molecules to get closer together which increases the electrostatic and breaking up the droplets, which then forming ions in a process that is still not well understood [6].

The main advantage of ESI/MS over other MS techniques is that ESI/MS overcomes the propensity of many biomolecules to fragment following ionization and enables the formation of multiply charged ions. Thus, ESI/MS is critical for the detailed structural analysis of large biomolecules like eicosanoids, moreover it is not necessary to chemically modify eicosanoids to enhance ionization efficiently when using this technique [6].

Ion traps are normally coupled to ESI ionization source for the structural characterization of eicosanoids as a mass analyzer, the ion trap uses an oscillating electric field to trap ions.

Ion trap mass analyzers exhibit high sensitivity and are most strongly characterized by the ability to perform multiple stages of mass spectrometry (MS^n). Up to 12 stages of tandem mass spectrometry (MS^{12}) have been performed using an ion trap, which greatly increases the amount of structural information obtainable for a given molecule.

An overview of the published methods for analysis of eicosanoids in biological tissues revealed that the main focus has been on brain, lung, liver and colon (Table 1.2). One important feature of the overview presented in Table 1.2 is the scarcity of methods for determining eicosanoids

in fish. The majority of studies presented in Table 1.2 are focused on both human and rodents [6].

Figure 1.3 shows an overview of the application of different analytical techniques for the analysis of eicosanoids in solid tissue over the last 30 years, LC/MS has become the main technique to analyze eicosanoids the last decade due to the multiple improvements introduced in that technique, it is also notable that ultra-performance liquid chromatography UPLC has been introduced in the last 10 years as possible technique of choice.

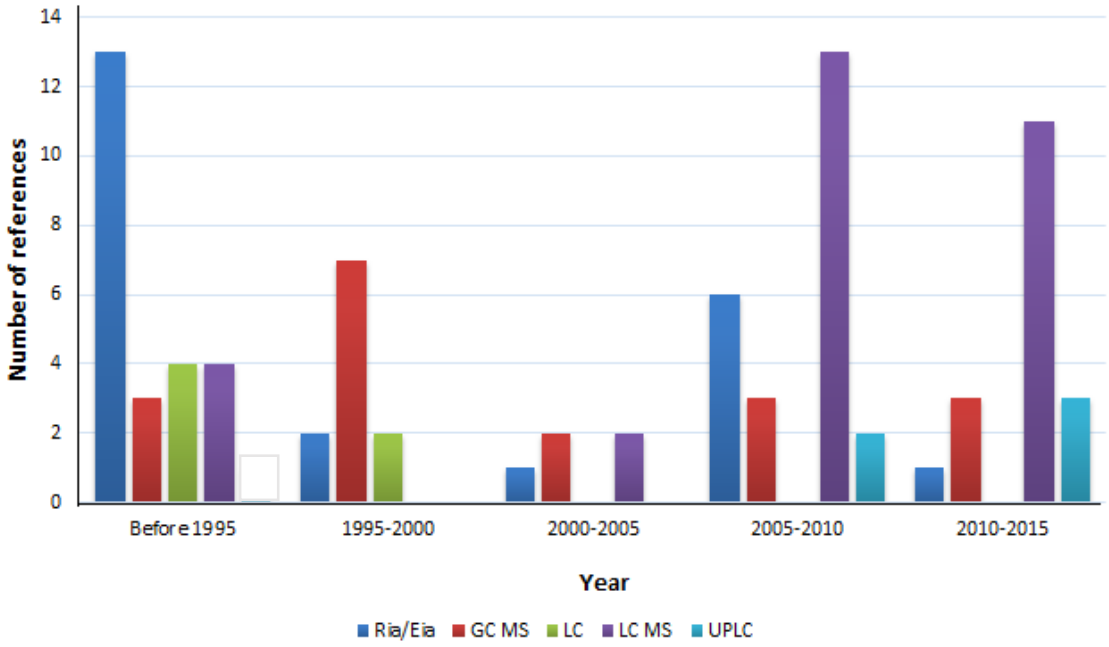

Figure 1.3 An overview of the application of different analytical techniques for the analysis of eicosanoids in solid tissue over the last 30 years**.**

1.2.2 Chemical structure of eicosanoids and fragmentation patterns

The analyzed eicosanoids in this thesis are PGE_2 and LTB_4 and their corresponding deuterated analogs PGE_2-d_4 and LTB_4-d_4. Their chemical structures are shown in Figure 1.4.

It is worth to mention that PGE_2 and LTB_4 have two and four double bonds respectively which explains the numbers in their abbreviated names [82].

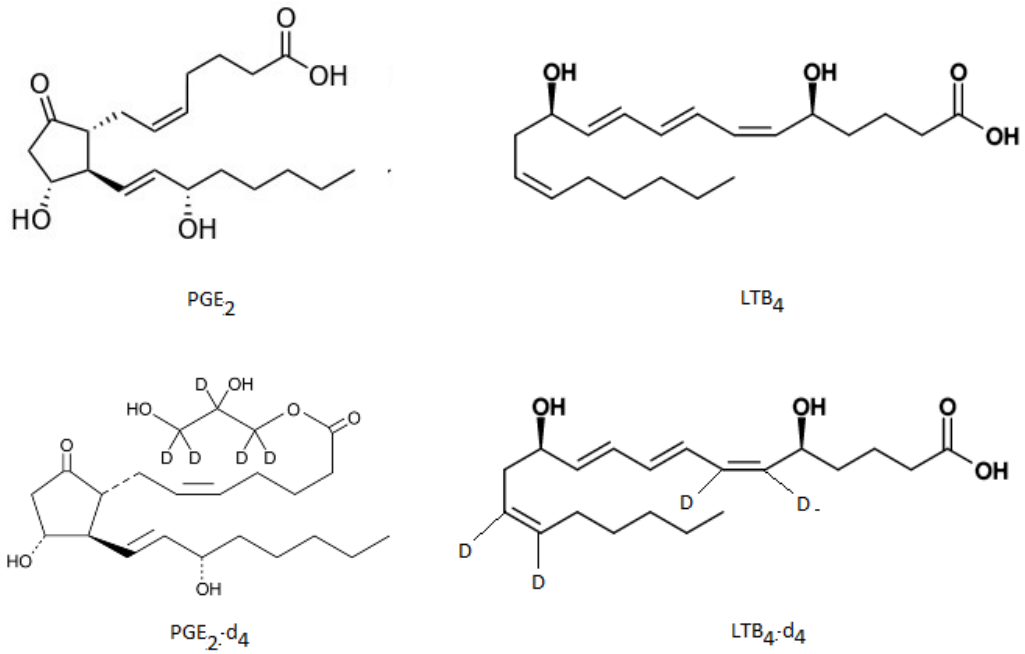

Figure 1.4 Chemical structure eicosanoids analyzed in this thesis and their corresponding internal standards

The typical ion fragments of the studied eicosanoids in negative mode are shown in Table 1.3. The deuterated internal standards, PGE_2-d_4 (356 Daltons) and LTB_4-d_4 (340 Daltons), are fragmented in a similar fashion [82].

Table 1.3 the parent ion and the ion fragment for PGE_2 and LTB_4

Eicosanoid	Parent ion m/z	Product ions m/z	Corresponding products
$PGE_2/PGE_2\text{-}d_4$	351/355 $[M^*\text{-}H]^-$	333/337	$[M\text{-}H_2O\text{-}H]^-$
		317/321	$[M\text{-}2H_2O\text{-}H]^-$
		271/275	$[M\text{-}2H_2O\text{-}CO_2\text{-}H]^-$
LTB_4	335/339$[M^*\text{-}H]^-$	315/319	$[M\text{-}H_2O\text{-}H]^-$
		299/303	$[M\text{-}2H_2O\text{-}H]^-$
		273/377	$[M\text{-}H_2O\text{-}CO_2\text{-}H]^-$
		195/197	$[M\text{-}C_9H_{17}O\text{-}H]^-$

*****M is the precursor molecule.

1.2.3 Eicosanoids extraction

The first step in eicosanoids analysis involves the collection of biological samples from human or animal subjects. These samples can be solid in nature (tissue) or comprise highly complex biofluids (e.g., plasma, serum, urine) [9]. In general, the sample-preparation protocol for tissues is more labor intensive and complex than for bio-fluids, due to the need for additional disruption and homogenization steps of tissues or cells prior to eicosanoids extraction.

A typical protocol commences with the sample being rapidly flash-frozen in liquid nitrogen, prior to storage at very low temperatures (around -80°C). This step helps to inhibit enzymatic activity and to reduce the rate of oxidation, peroxidation and hydrolytic degradation of lipids containing unsaturated bonds like eicosanoids [9].

Strategies for sample clean-up and concentration in eicosanoid analysis range from solid-phase extraction (SPE) over liquid extraction (LE) to protein precipitation to simple solvent extraction, with SPE being the most frequently used technique, as shown in Table 1.4 [9].

SPE is a popular method for eicosanoid analysis since it is easy to perform, fast, and it cleans up interfering matrix without the need to increase the temperature or to use external energy.

Nevertheless, it has some disadvantages, such as high cost of the cartridges, and the need to use of toxic organic solvents with detrimental effects towards humans and the environment [9]. Solvents used for LE of eicosanoids include hexane–ethyl acetate, chloroform–ethyl acetate, 2-propanol–hexane, or methanol–chloroform while protein precipitation is applied in protocols for plasma sample clean-up alone or prior to SPE.

The main advantages of LE are: it is simple and easy to perform; the low cost solvent used as well as the apparatus; no need to use external energy or high temperature; short extraction time [9]. However, as shown in Table 1.4, LE has been less used for the extraction of eicosanoids from solid tissue due to the complexity of the tissues which is reflected in Table 1.4 by the low number of published LE methods compared to SPE methods.

Table 1.4: Overview of the extraction methods different instrumental techniques of eicosanoids in tissues prior to chromatography based methods.

	SPE	LE
Number of methods	**23** [12, 13, 15, 16, 19, 22, 25-27, 29, 32, 33, 35, 37, 44-46, 53, 55, 56, 60, 66, 78]	**10** [14, 22, 30, 36, 54, 68, 71, 77, 81, 82]

Corresponding references are given in square brackets

1.3 Thesis objectives

The main objective of the present master thesis is to develop a liquid extraction method for determining PGE_2 and LTB_4 in fish liver by means of LC-MS/MS. To this aim the following task are proposed:

1- Application of a mixture design to select the optimal solvent combination for extracting PGE_2 and LTB_4 from salmon liver samples.

2- Determination of the optimal concentrations of internal standards, specifically PGE_2-d_4 and LTB_4-d_4, by using a Doehlert uniform shell design.

3- Validation of the developed method with emphasis on selectivity, linearity, precision, accuracy, limit of detection, limit of quantification, stability and range.

2. Selection of the extraction system

2.1 Mixture design

Previous studies have shown that the best solvent combination for extracting prostaglandins from fish gonads is acetonitrile and chloroform (1:1) [67]. In addition, another study of the determination of prostaglandins and leukotrienes in human plasma has suggested the addition of formic acid before the extraction step in order to avoid protein precipitation [83].
However, the optimal combination of these solvents for the extraction of eicosanoid from salmon liver needs to be determined.

A Mixture design of the type simplex lattice design was chosen to identify the optimum extraction mixture [84]. The proportion of the selected solvents rather than the amount of the used solvents was the main interest. The proportions of the three solvents must sum up to 1 satisfying the constraint:

$$S1 + S2 + S3 = 1.0 \qquad (2.1)$$

Where S1 is chloroform, S2 is formic acid and S3 is acetonitrile.

Thus the proportions of solvents must be adjusted to render a total volume of the extraction solution of 1000 µL.

The used simplex lattice designed is presented in Figure 2.1. Simplex lattice design defines the optimum mixture by estimating the response surface over the simplex region, this could be done by choosing 10 points (A to J) evenly spread over the whole triangle and each point representing a particular solvent mixture where the extraction procedure is implemented.

The points A, H and J in Figure 2.1 involve single solvent (acetonitrile, formic acid and chloroform respectively). Point E represents the centroid point (equal proportion of the three solvents), and the selected points C, D and I are located along each side of the triangle and characterized by equal proportions of two solvents while the interior points of the triangle B, F and G are characterized by different mixture of three solvents.

Table 2.1 describes all the selected points (A, B, C, …, J) with the corresponding volume of solvents in microliters (µL).

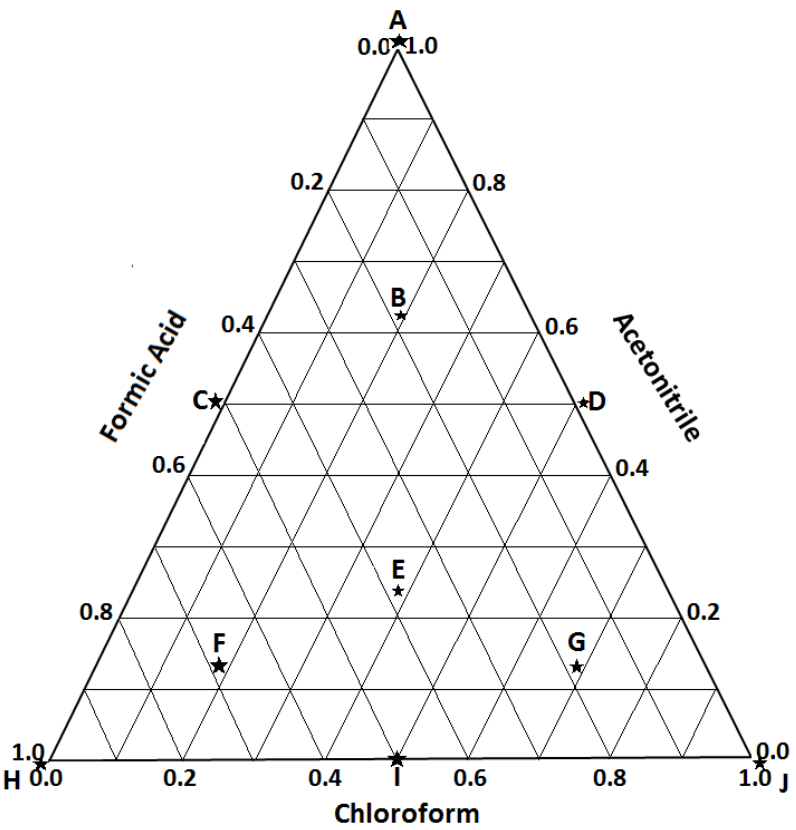

Figure 2.1 selected points for solvent mixture design

Table 2.1 Volume of solvents used in connection with the simplex design portrayed in Figure 2.1

Experiment	Formic	Chloroform	Acetonitrile
A	0	0	1000
B	170	170	660
C	500	0	500
D	0	500	500
E	330	330	330
F	660	170	170
G	170	660	170
H	1000	0	0
I	500	500	0
J	0	1000	0

2.2 Experimental

2.2.1 Reagents.

Acetonitrile (liquid chromatographic grade, 99.8%) and formic acid (98%) were obtained from Sigma-Aldrich (USA). And chloroform (liquid chromatographic grade, 99.8%) was purchased from Merck (Germany). Liquid nitrogen and dry ice were provided by Tess (Norway).

2.2.2 Extraction procedure

A wild salmon liver sample stored at -80 °C was crushed to fine powder and homogenized as follows: a thick and heavy mortar, previously cooled down with liquid nitrogen, was placed in a styrofoam box containing 1 kg of dry ice. The dry ice was placed in a layer on the bottom and the mortar on top of it, then the liver sample was placed in the mortar and pulverized by using a pestle. Liquid nitrogen was added to the sample to keep the sample frozen during the pulverization procedure.

The pulverized sample was homogenized by a spatula and distributed in portions of 300 µg in ten plastic tubes and immediately stored at −80 °C until extraction.

The ten solvent combinations described in Table 2.1 were added to the ten tubes containing 300 µg of homogenized salmon liver. The tubes were vortex-mixed for 1 min, centrifuged at 6037×g for 1 min, the supernatant collected in test tubes using a Pasteur pipet and the extraction

procedure repeated on the remaining flocks from the initially extracted tubes. The supernatants of the second extraction are pooled with their corresponding initially collected supernatants, dried under nitrogen gas, diluted to 100 µL with acetonitrile, centrifuged at 6037×g for 1 min and submitted to LC-MS/MS analysis after confirming lack of precipitation visually.
It must be mentioned that due to the sample limitation, the experiments were performed in duplicate.

2.2.3 Liquid chromatography – Mass spectrometry LC/MS

The LC/MS was an Agilent 1100 series LC/MSD trap, SL model with an electrospray interface (ESI), the injection volume was set to be 25 µL and 30 minutes total analysis time. The column used was a Zorbax Eclipse-C8 RP 150 mm×4.6 mm, 5µm (Agilent Technologies, Palo Alto, CA, USA) kept at 50 °C. The mobile phase operated in isocratic mode was acetonitrile with 0.1% (v/v) formic acid at a flow rate of at 0.2 mL/min and UV detection at 254 nm.
Nitrogen was used as nebulizer and drying gas at 350 °C. The ESI source was operated in negative ion mode and the ion optics responsible for getting the ions in the ion-trap such as capillary exit, skimmer, lens and octapoles voltages were controlled by using the Smart View option with a resolution of 13,000 m/z s^{-1}.
Complete system control, data acquisition and processing were done using the ChemStation for LC-MSD Trap Software, Version 5.3 from © Agilent Technologies, Inc., 2005. The analytical eicosanoids were isolated as $[M-H]^-$ ions (M = PGE_2 and LTB_4) and the characteristic fragment ions used for qualification purposes are referred in Table 1.3The monitored transitions were : m/z 351→333, 315, 271 for PGE_2 and m/z 335→317, 299, 273, 255, 195 for LTB_4. The summation of the extracted ion chromatogram (EIC) intensities of the characteristic fragments, in ion counts per second, were computed for quantification purposes.

2.2.4 Selection criteria for the optimal extraction system

The selection of the best extraction solvent composition was based on visual inspection of the supernatants and the strength of the analytical signals of the ten extractions systems described in Figure 2.1. The best extraction systems were those exhibiting clearest and brightest supernatants and the highest extracted ion chromatogram (EIC) peak areas in ion captured per second.
All of the calculation were carried out in Excel (Microsoft Office Excel 2010).

2.3 Results and discussion

The physical appearance of the ten supernatants obtained after performing the ten extractions suggested in Figure 2.1 are described in Table 2.2.

Table 2.2 Physical appearance of the supernatants after treating the salmon liver with the solvents composition indicated in Figure 2.1

Tube*	Color of the solution	Physical appearance
A	Transparent	Clear supernatant
B	Red	Thick precipitated layer and no supernatant produced
C	Dark brown	Not clear supernatant, Burned-like extract
D	Yellow	Clear liquid oily supernatant
E	Red	Not clear supernatant, visible precipitation
F	Light brown	Not clear supernatant, milky solution.
G	Brown	Clear supernatant, visible precipitated layer
H	Red	Not clear supernatant, visible precipitation
I	Orange	Not clear supernatant, visible precipitation
J	Transparent	visible precipitation

***** Tube letter corresponds to the letters indicated in Figure 2.1

As noticed from the Table 2.2 all samples B, C, E, F, and H, were not measured instrumentally due to the persistency of turbidity after centrifugation, this might be due to the use of pure formic acid (99%) which burned the fish tissue. Only the clear and bright supernatants without any visible particles (Systems A, D and G) were injected.

The total ion chromatograms (TIC) for the systems A, D and G are shown in Figure 2.2.

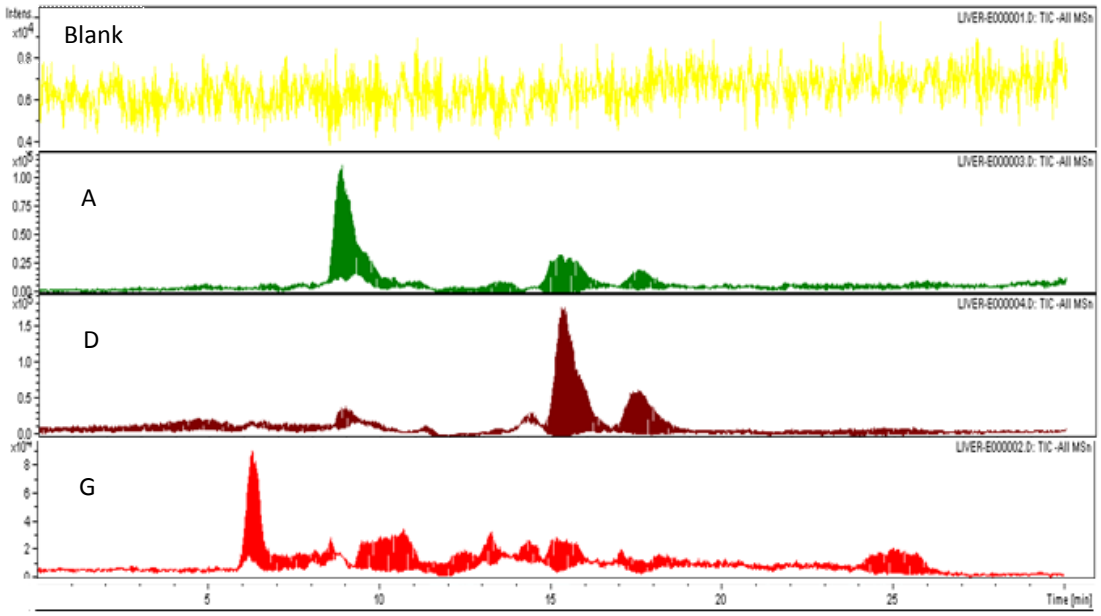

Figure 2.2 TIC corresponding to the Blank and one sample of each extraction system A, D, and G

Table 2.3 shows peak areas of extracted ion chromatogram EIC that correspond to injected samples, extraction system G, characterized by the use of equal fraction of three solvents in the solvent mixture, exhibited the highest relative standards deviation RSD for both LTB_4 and PGE_2. Acetonitrile did not exhibit any instrumental signal for neither PGE_2 nor LTB_4 when used as a blank

Figure 2.3 shows that the extraction systems A and D produced different TIC. However, Table 2.3 and Figure 2.3, describing the EIC for A and D, revealed that both systems generated approximately similar signals and accepted RSD (<15%).

The comparison of the PGE_2 signal for the extraction system A and D showed a consistent slightly higher intensity for the latter system (Figure 2.4). Furthermore, the extraction system D was selected as the optimal system for extracting eicosanoids from salmon liver. These results are in agreement with those reported elsewhere [1]. System G was discarded due to the high relative standard deviations (Table 2.3).

Table 2.3 EIC peak area corresponding to the three extraction system for PGE_2 and LTB_4.

Extraction systems	PGE_2		LTB_4	
	Mean	RSD %	Mean	RSD %
A	132922	8.2	93650	1.7
D	139880	13.4	86984	13
G	164612	51.6	117194	84994

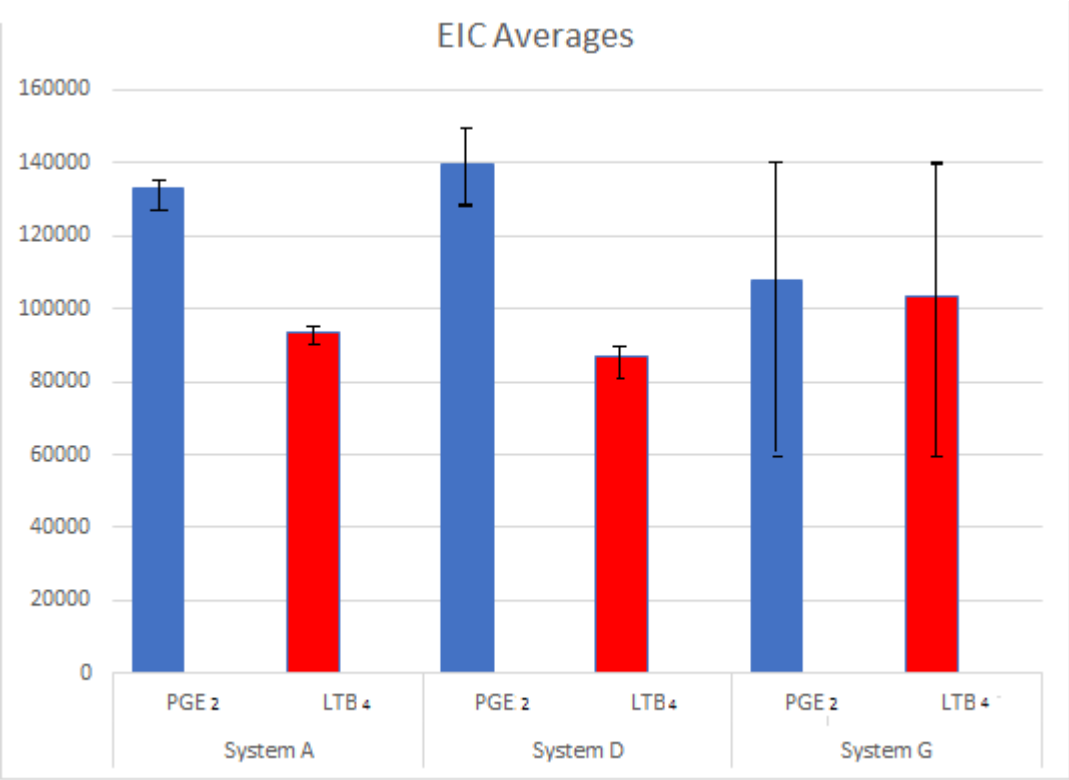

Figure 2.4 EIC peak area averages for both PGE_2 and LTB_4 corresponding to the three extraction systems

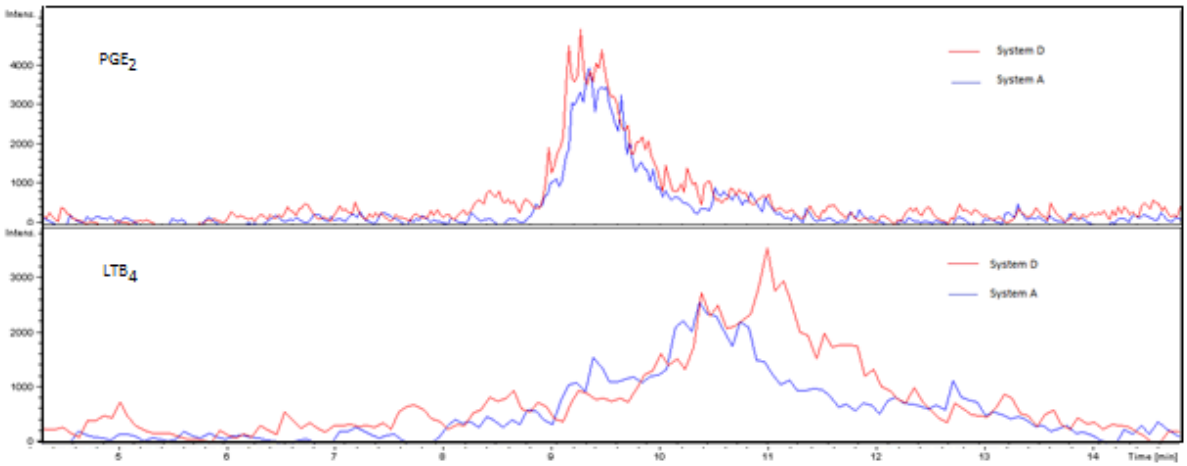

Figure 2.4 Monitored extracted ion chromatogram signals for PGE_2 and LTB_4.

The retention times for PGE_2 and LTB_4 were 9.3 min and 11 min respectively, and the corresponding mass spectra of both target analytes extracted using the system D is shown in Figure 2.5.

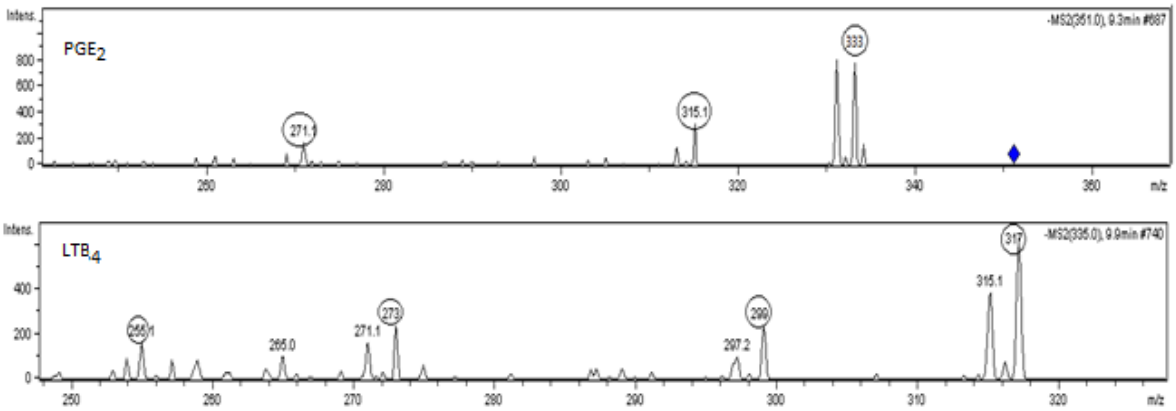

Figure 2.5 fragmentation patterns for PGE_2 and LTB_4 using the extraction system D.

2.4 Conclusions

Based on the clarity and brightness of the supernatant and signal intensities, the extraction system D, consisting of equal amounts of acetonitrile and chloroform (500 µL of each) was selected as the optimal solvent composition for extracting PGE_2 and LTB_4 from salmon liver upon the 10 extraction systems investigated. The addition of formic acid dissolved the liver tissue and generated turbidity, thus formic has been ruled out.

The implementation of a simplex lattice design has demonstrated to be a reliable strategy not only for selecting the optimal combination of solvents but also for guiding the analyst in the rational selection of potential experimental conditions.

3. Optimization of internal standard addition

3.1 Selection of the optimal concentrations of internal standards.

3.1.1 Response Factor

In order to assist quantification in LC/MS systems, it is common to use an internal standard with a similar chemical structure and properties to that of the analyte of interest. This involves preparation of solution of known concentration of analyte [A] spiked with known concentration of internal standard [IS], then determination of their signal ratio (S_A/S_{IS}) and their response factor (*RF*) computed as:

$$RF = \frac{S_A}{S_{IS}} \times \frac{[IS]}{[A]} \qquad (3.1)$$

Therefore, once *RF* is determined at a given known concentration of spiked IS, the unknown concentration of the analyte can be calculated from their response signals, assuming that the two factors ([A] and [IS]) exhibit a linear relationship towards the detector over the studied range of concentrations. Traditionally, details on the detector linearity are commonly described for the analyte alone or in combination with a fixed amount of internal standard, and no description is given on how to estimate the best level of internal standard [83].

The *RF* of the internal standard can remain constant or it may vary dramatically over the analytical range, The reason could be related to the degree of ionization of the internal standard in the electrospray ion source and the interaction between analyte and internal standard [85]. Thus the *RF* and also the accuracy of the determination require optimization of both concentration ranges (analytes and internal standards) in order to assure constant *RF* values throughout the analytical ranges. Some researchers have been pointed out that more comprehensive studies on how simultaneous changes of the analyte and the internal standard affect the response factor *RF* and therefore, the quantification process, need to be performed. [85]

3.1.2 Experimental design in quantification experiments.

Several techniques are commonly used in the estimation of an optimal level of internal standard and further calculation of *RF*. For instance, it has been suggested that the analysis of one or two levels of internal standard and three levels of analyte is appropriate in order to estimate a reliable amount of the former and to build an appropriate curve of the latter [85, 86]. Another approach

is to target the internal standard to the lower 1/3 of the working standard curve in order to have a level above the limit of quantification but not so high as to overshadow the analytical signal [87].

These approaches do not consider the dependence of the response of the internal standard on the concentration of the analyte. Consequently, the determination of the dependence of these factors is essential. Different models and experimental designs can be used in order to study the behavior of *RF* when [A] and [IS] are varied. The main characteristics and properties of various experimental designs are shown in Table 3.1.

The models described by the different experimental arrangements are:

$$RF = b_0 + b_A[\mathrm{A}] + b_{IS}[\mathrm{IS}] \qquad (3.2)$$

$$RF = b_0 + b_A[\mathrm{A}] + b_{IS}[\mathrm{IS}] + b_{A\times IS}[\mathrm{A}] \times [\mathrm{IS}] \qquad (3.3)$$

$$RF = b_0 + b_A[\mathrm{A}] + b_{IS}[\mathrm{IS}] + b_A{}^2[\mathrm{A}]^2 + b^2{}_{IS}[\mathrm{IS}]^2 + b_{A\times IS}[\mathrm{A}]\times[\mathrm{IS}] \qquad (3.4)$$

Where b_0 represents the intercept, b_A and b_{IS} the linear term coefficients, $b_{A\times IS}$ the first order interaction effect coefficient and $b^2{}_A$ and $b^2{}_{IS}$ are second order curvature effect coefficients.

The number of degrees of freedom is an important parameter that should be considered when judging the lack of fit of a model the degrees of freedom in Table 3.1 are defined as the minimum number of experiments minus the number of parameter in the model. The term efficiency (E) in Table 3.1 which measures the relationship between the number of estimated coefficients and the amount of effort put into the execution of the experiments is defined by the expression:

$$E = \frac{\text{number of coefficients}}{\text{number of experiments}} \qquad (3.5)$$

In quantification experiments aiming at studying the behavior of *RF* and the optimal amount of internal standard, values of E lying between 0.40 and 0.60 can be considered acceptable.

Table 3.1 Main characteristics of the various experimental designs discussed in this section*

Design	Type	Experimental arrangement	Minimum number of experiments for N=2 variables	Number of [A]levels	Number of [IS]levels	Model	Degrees of freedom	Efficiency
Factorial	2 levels	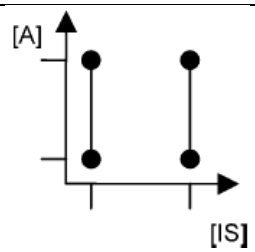	2^N = 4 exp	2	2	Eq. (3.2) Eq. (3.3)	1 0	0,75 1
	3 levels	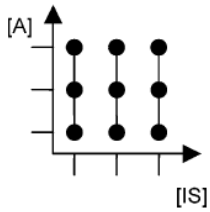	3^N = 9 exp	3	3	Eq. (3.2) Eq. (3.3) Eq. (3.4)	6 5 3	0.33 0.44 0.67
Sequential	Simplex	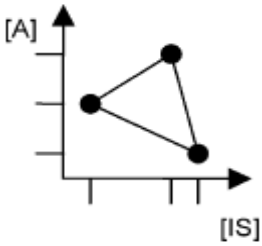	N+1=3 exp	3	3	Eq. (3.2)	0	1
	Star	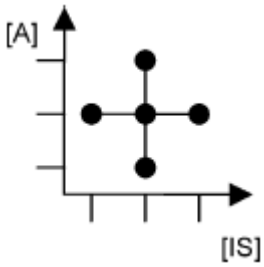	2N+1=5 exp	3	3	Eq. (3.2) Eq. (3.4)	2 0	0.6 1
Simultaneous	Central composite	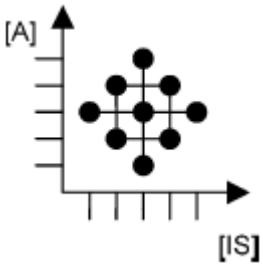	2^N+2N+1=9 exp	5	5	Eq. (3.2) Eq. (3.3) Eq. (3.4)	6 5 3	0.33 0.44 0.67

Uniform shell	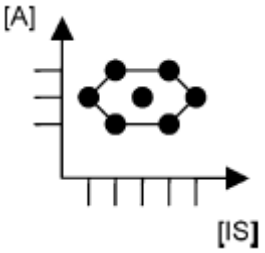	$2^N+N+1=7$ exp	3	5	Eq. (3.2)	4	0.43
					Eq. (3.3)	3	0.57
					Eq. (3.4)	1	0.86

* Table adopted from *Analyst*, **1997**, *122*, 621–630.

Factorial design seems a simple and adequate approach to model the effect of the two variables with a minimum number of experiments. However, the disadvantages of this design are the few levels of analyte and internal standard studied and the lack of degree of freedom to estimate the lack of fit errors. Higher level factorial design is not advisable due to the low number of concentration levels studied compared to the high number of experiments performed [85].

Simplex designs are limited by the lack of degree of freedom when a minimum number of experiments is considered. Star design offers a reasonable number of experiments, concentration levels and degrees of freedom although they cannot estimate first order interaction effects A central composite design adding four more experiments and providing more concentration levels can overcome this.

Uniform shell design, specifically a Doehlert design [88], allows the study of the same number of models as the central composite design with a minimum number of experiments, allocated in a regular hexagon with a point in the center (Figure 3.1). The design generates information equally spaced in all directions since the experimental points are equally distributed on the surface of spherical shell and each point in the design has equal distance to the center as well to its neighbor experimental points (Figure 3.2a). In addition, it is possible to extend the experimental matrix and study other experimental arrangements by using previous experiments (Figure 3.2b).

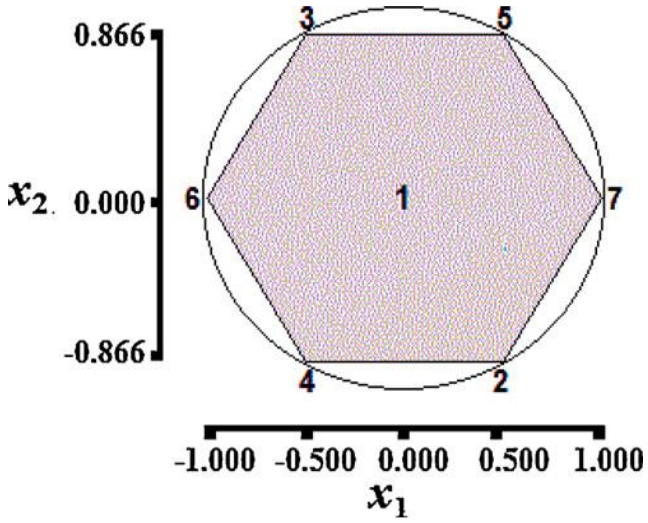

Figure 3.1 The two-factor (x_1, x_2) Doehlert design. The design has the five experimental levels along x_1 dimension with coded value -1.00, -0.50, 0.00, 0.50 and 1.00 respectively. Similarly the three experimental levels along x_2 dimension have coded value -0.866, 0.000 and 0.866 respectively.

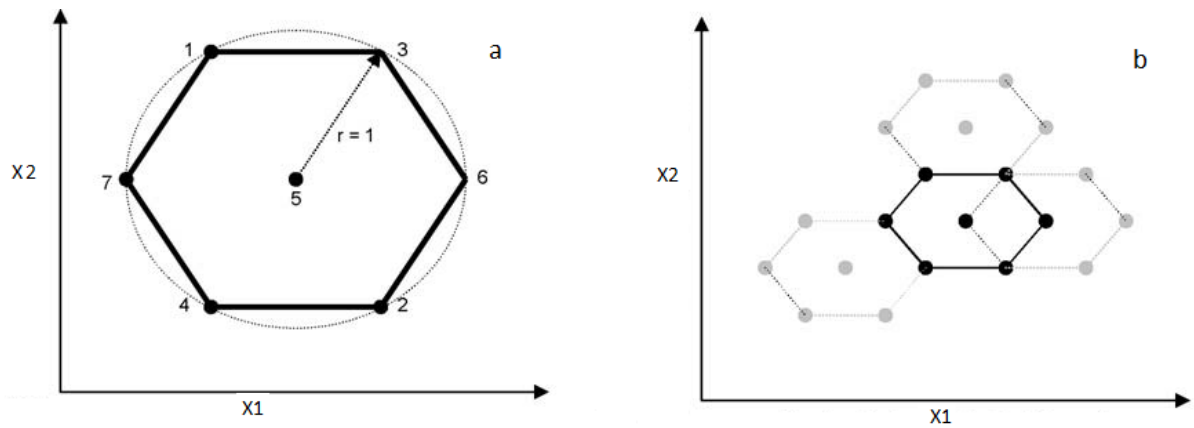

Figure 3.2 Doelhert design properties: **a.** spatial distribution of the experimental points; **b.** extension of the initial matrix by using previous adjacent points.

One characteristic of this type of design is the unequal number of experimental levels at the different axes. When studying two factors, one factor is varied over three levels while the other is varied over 5 levels, as can be seen from figure 3.2a. This is an important feature, as there are often cases where the factors under study are subjected to different ranges and levels and to avoid unnecessary experiments [83].

3.1.3 Number of replicates

In quantification experiments, where the preparation error is always larger than the instrumental error, the use of replicates is essential in order to decrease the associated errors [89]. Uncertainty of an experimental design measures how confidently a model predicts data in an experimental region; the greater uncertainty indicates less confidence in the predictions. For a given experiment, *i*, in a design matrix $\boldsymbol{X}$, the uncertainty can be defined by:

$$U_n^2 = s_e^2\ [1+\boldsymbol{x}_i(\boldsymbol{X}'\boldsymbol{X})^{-1}\boldsymbol{x}_i'] \qquad (3.6)$$

Where s_e is the squared residual error over the total number of experiments *N*. The term $\boldsymbol{x}_i\,(\boldsymbol{X}'\boldsymbol{X})^{-1}\boldsymbol{x}_i$ depends only on the design and not on the experimental response, so it is possible to predict the uncertainty without performing any experiment by changing the levels of the variable x_i across the domain of the factor space [89].

When several replicates are introduced in the design matrix, the uncertainty of prediction of the mean of q values (where q is the number of the replicates) is given by:

$$U_n^2 = s_e^2\,[1/q + \boldsymbol{x}_i\,(\boldsymbol{X}'\boldsymbol{X})^{-1}\boldsymbol{x}_i'] \qquad (3.7)$$

The equation (3.7) shows that uncertainty of an experimental design is influenced by the number of replicates, so it is important to determine in advance the number of replicates [89]. The number of replicate in the design matrix also affects the term $\boldsymbol{x}_i\,(\boldsymbol{X}'\boldsymbol{X})^{-1}\boldsymbol{x}_i$ as it will explained in the next section.

3.1.4 Leverage

The term $\boldsymbol{x}_i\,(\boldsymbol{X}'\boldsymbol{X})^{-1}\boldsymbol{x}_i$ is a measure of the potential influence of an observation on the parameter estimated and is usually called Leverage, h [89].

The leverage can be calculated to show how confidence changes when the design or model is altered.

The Matrix $\mathbf{H}= \boldsymbol{X}(\boldsymbol{X}'\boldsymbol{X})^{-1}\boldsymbol{X}'$ is called the hat matrix and it has the property that its diagonal elements equal the leverage at each experimental point [89]. Tables 3.2 and 3.3 show the design matrix and the hat matrix for a central composite design respectively when two factors in triplicate (q=3) are considered.

The sum of leverage over all experimental points equals the number of coefficients in the model, thus the more replicates used the smaller the leverage is, For instance, the model proposed in (Eq. 3.2) involves three coefficients, so the hat matrix of the previous design example presented in Table 3.3 will demonstrate that no matter how many experiments are carried out, the summation over all the diagonal elements of the hat matrix will always be three, therefore introducing more replicates in the design matrix will reduce the leverage and thus reduce the uncertainty in the proposed model. Also, as shown in Table 3.2, the leverage is less in the region where the experimental points are close to the center and the leverage has equal value over all the points that has the same distance from the center.

In the uniform shell design (Figure 3.1), all the experimental points (except the center points) have the same uncertainty since it has the same distance from the center point, unlike other types of the designs where the uncertainty varies between experimental points.

Table 3.2 Central composite design matrix used as example to calculate the leverage matrix where 5 levels of the variables x_1 and x_2 are considered, and b in the intercept.

Experiment number	b	x_1	x_2
1	1	-2	0
2	1	-1	1
3	1	-1	-1
4	1	0	0
5	1	0	2
6	1	0	-2
7	1	1	1
8	1	1	-1
9	1	2	0

Table 3.3 Computation of the hat matrix $\boldsymbol{X}(\boldsymbol{X}'\boldsymbol{X})^{-1}\boldsymbol{X}'$ for the design matrix given in Table 3.2

0,44	0,28	0,28	0,11	0,11	0,11	-0,06	-0,06	-0,22
0,28	0,28	0,11	0,11	0,28	-0,06	0,11	-0,06	-0,06
0,28	0,11	0,28	0,11	-0,06	0,28	-0,06	0,11	-0,06
0,11	0,11	0,11	0,11	0,11	0,11	0,11	0,11	0,11
0,11	0,28	-0,06	0,11	0,44	-0,22	0,28	-0,06	0,11
0,11	-0,06	0,28	0,11	-0,22	0,44	-0,06	0,28	0,11
-0,06	0,11	-0,06	0,11	0,28	-0,06	0,28	0,11	0,28
-0,06	-0,06	0,11	0,11	-0,06	0,28	0,11	0,28	0,28
-0,22	-0,06	-0,06	0,11	0,11	0,11	0,28	0,28	0,44

Star design points leverage value

Central point leverage value

Factorial design points leverage value

A comparison between different types of design in terms of the highest and the lowest uncertainty is shown in the table 3.4. The comparison shows that the uncertainty decreases when the number of replicates in the design matrix increases. Although the central composite design has the lowest uncertainty, the high number of experiments favors the uniform shell design.

Table 3.4 comparison between different types of design in terms of the highest and the lowest uncertainty.

Design Type	Number of experiments	Highest uncertainty	Lowest uncertainty	Comment
Simplex	3	1,000	1	3 experimental points
	6	0,500	0,5000	3 duplicated experimental points
	15	0,200	0,2000	3 triplicated experimental points
Star	5	0,7000	0,2000	5 experimental points
	10	0,3500	0,1000	5 duplicated experimental points
	15	0,2330	0,6660	5 triplicated experimental points
Central composite	9	0,4440	0,1110	9 experimental points
	18	0,2220	0,0556	9 duplicated experimental points
	27	0,1480	0,0370	9 triplicated experimental points
Uniform shell	7	0,4760	0,1420	7 experimental points
	14	0,2380	0,0710	7 duplicated experimental points
	21	0,1580	0,0476	7 duplicated experimental points
	15	0,2333	0,0660	7 duplicated experimental points with one and two triplicated experiments
	17	0,2150	0,0582	

Figures 3.3 and 3.4 show the changes in the uncertainty associated with central composite designs and uniform shell design respectively when different number of replicates are used.

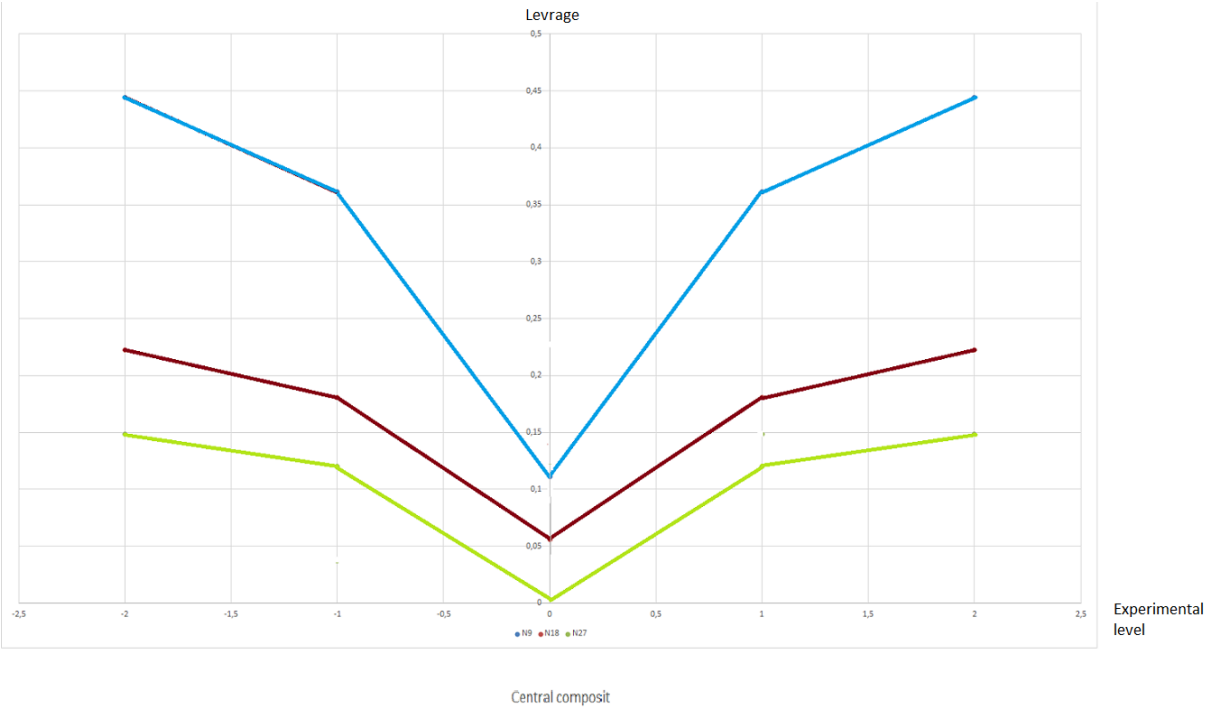

Figure 3.3 Changes in uncertainty in a central composite designs when different number of replicates are introduced.

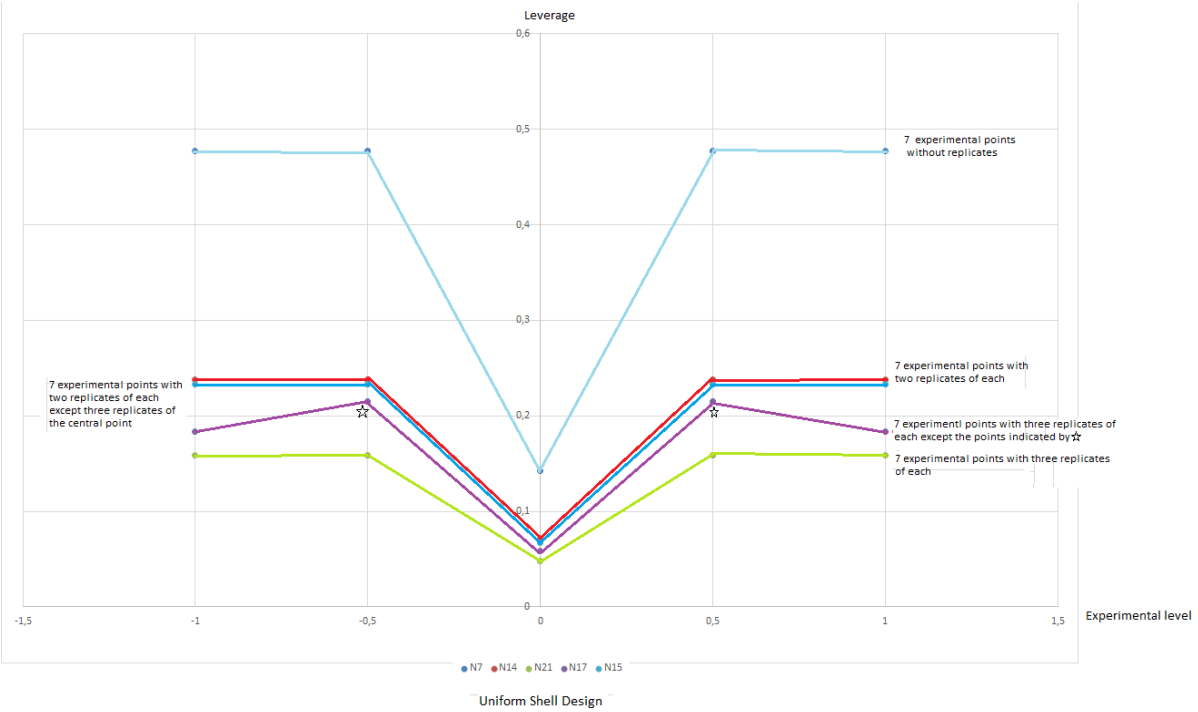

Figure 3.4 The changes in the uncertainty associated with uniform shell design when different number of replicate used.

A comparison between Figures 3.3 and 3.4 allows concluding that a Doehlert design is an optimal strategy for optimizing the amount of internal standard to be used in connection with the analysis of eicosanoids in salmon liver. In addition, a close inspection of Figure 3.4, shows that the best replication regimes, with the lowest uncertainty, are those represented by the green and purple traces, corresponding to a total of 21 and 17 experiments respectively.

3.1.5 Selection of the design

The uniform shell design of 17 experiments described in Figure 3.4 (purple trace) was the selected choice in terms of the relative low number of experiments. The matrix with 21 experiments was not considered due to the fact that the uncertainty (green trace in Figure 3.4) did not much decrease when introducing 4 more experiments (n=17+4).

Since a blank sample (wild salmon liver with an undetectable level of eicosaoinds) was not available, 3 more experimental points that involve the addition of 3 different levels of internal standard to estimate the endogenous level of eicosanoid in the liver sample were added. The extra points in questions are represented in Figure 3.5 with a red circle. The final design matrix is described in Table 3.5.

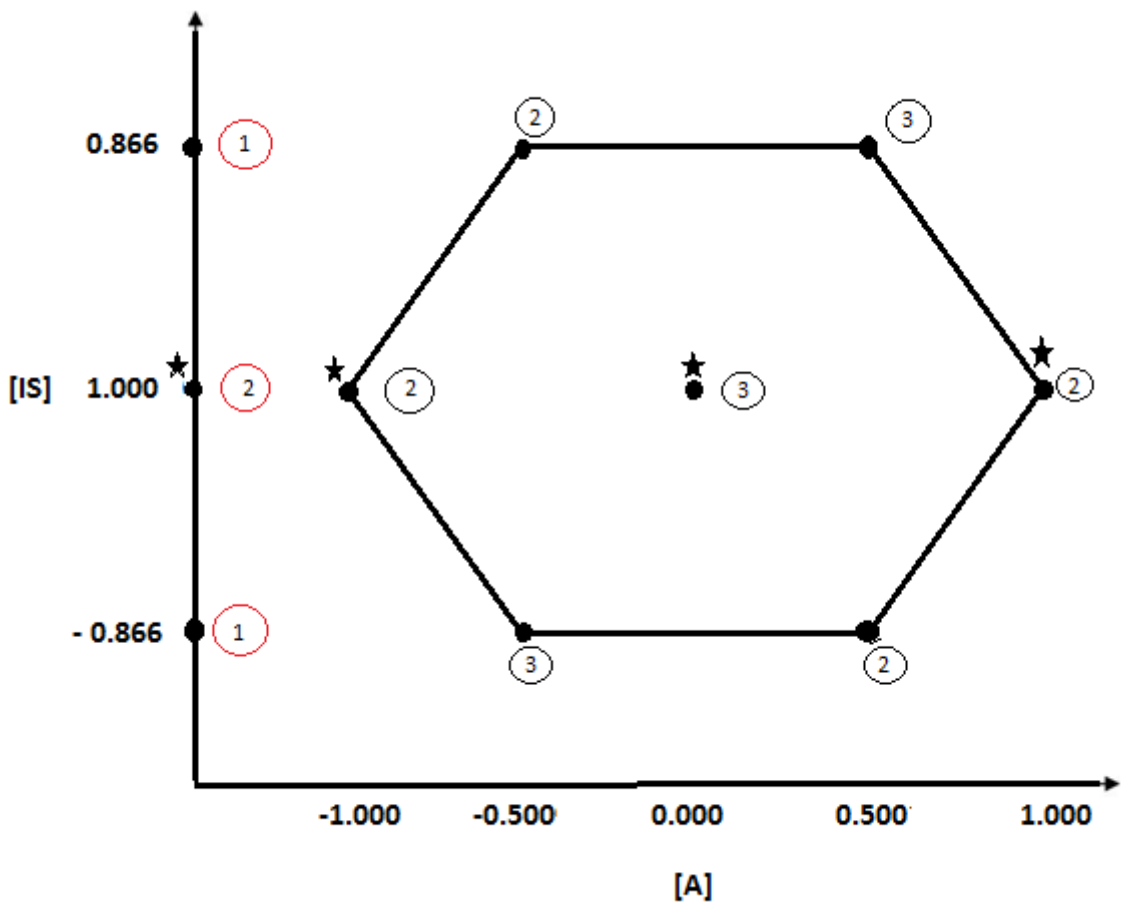

Figure 3.5: Selected experimental points to estimate the response factor.
Black circles corresponds to uniform shell design experimental points, while red circles indicate samples only spiked with internal standard, also, the number in the circle indicates the number of replicates.
Experimental points marked with stars correspond to standard addition method experimental points.

Levels of PGE_2 in different fish tissues (e.g. brain, kidney and heart) have been reported to be up to 50 pg/mg [90, 91]. Based on this concentration, the investigated analytical range for both PGE_2 and LTB_4 was set to be 1-50 ng/g.

The studied range for the PGE_2-d_4 and LTB_4-d_4 was sat to be 15-50 ng/g assuming that the level of internal standard addition should be above the lower 1/3 of the working analyte range.

Table 3.5 the selected design matrix to estimate the response factor and the endogenous eicosanoids concentration

Experiment No.	Coded level		Natural level (ng/g)			
	x_1	x_2	x_1		x_2	
			PGE_2	LTB_4	PGE_2-d_4	LTB_4-d_4
1	0.0	00.00	25.00	25.00	32.5	32.5
2	0.5	-0.866	37.25	37.25	17.3	17.3
3	-0.5	0.866	13.20	13.20	47.7	47.7
4	-0.5	-0.866	13.20	13.20	17.3	17.3
5	0.5	0.866	37.25	37.25	47.7	47.7
6	-1.0	00.00	01.00	01.00	32.5	32.5
7	1.0	00.00	50.0	50.00	32.5	32.5
8	NP	-0.866	00.00	00.00	17.3	17.3
9	NP	00.00	00.00	00.00	32.5	32.5
10	NP	0.866	00.00	00.00	47.7	47.7

NP: not present

3.1.6 RF Modeling

RF behavior was studied and modeled by using Doehlert uniform shell design where the concentrations of the PGE_2 and LTB_4 with their respective deuterated internal standards were varied simultaneously (Table 3.5).

The *RF* was calculated by Eq. 3.1 at each of Doehlert design experimental points based on the obtained signal area of analyte and internal standard. Then the *RF* was explained or modeled based on the models in Eq. 3.4. The adequacy of the developed models was evaluated by the variance ratio test or Fisher ratio test (F-Test).

The F-test is a statistical parametric test commonly used to compare the lack-of-fit to pure error variances of a predetermined mathematical model. This statistical test is applied by calculating the variances of the lack-of-fit and pure errors by dividing their summation with respective degrees of freedom. The ratio of variance of the lack-of-fit error to that of pure error is known as experimental F-value (F_{Cal}) and used to conclude if the model fits the data by comparing with the theoretical (tabulated) F-value (F_{tab}). The process of an F-test can be seen in Table 3.6.

Table 3.6 The calculation of F test parameter to check the fitness of the model. *N*, *P*, *K* are the number of total experiments, number of regression coefficients and number of experimental points respectively.

Parameter	Equation
Variance of residual error (V_{RE})	$V_{RE} = \frac{\sum(RF_{exp} - RF_{cal})^2}{N-P}$
Variance of pure error (V_{PE})	$V_{PE} = \frac{\sum(RF_{exp} - \overline{RF})^2}{N-K}$
Variance of lack of fit (V_{LOF})	$V_{LOF} = \frac{\sum(RF_{cal} - \overline{RF})^2}{K-P}$
Calculated F (*cal*)	$F_{cal} = \frac{V_{LOF}}{V_{PE}}$

If F_{Cal} is less than F_{tab}, it means that the model explains the experimental data confidently. In some cases, it is possible to remove the non-significant regression coefficients in the Eq. 3.4 to increase the degrees of freedom and obtain a simpler model (reduced model). In this thesis, all the theoretical F-values were calculated at the 95 % confidence level of the F-distribution. Basic calculations, statistics and F-test were carried out in Excel 2010.

3.1.7 Estimation of endogeanous concentration by standard addition method.

The endogenous concentrations of PGE_2 and LTB_4 were estimated using the standard addition method, In this method, different amounts of standard are directly added to some aliquot of the sample and then the instrumental signal corresponding to these samples are determined. The results are plotted as shown in Figure 3.6, where the signal is plotted on the y-axis while the x-axis is graduated in terms of the concentration of analyte added. A regression line is estimated

and extrapolated to the point on the x-axis at which y = 0. This negative intercept on the x-axis corresponds to the amount of the analyte in the test sample [92].

In order to reduce errors related to the instrumental signal determination and systematic matrix effect, a constant amount of deuterated standard was added to each sample, and the signal of the analyte to the signal of the deuterated standard ratio S_A/S_{IS} was plotted on the y-axis. This methodology is particularly recommended in procedures for pesticide or drug residue analysis and other contaminants in food and biological matrices [93].

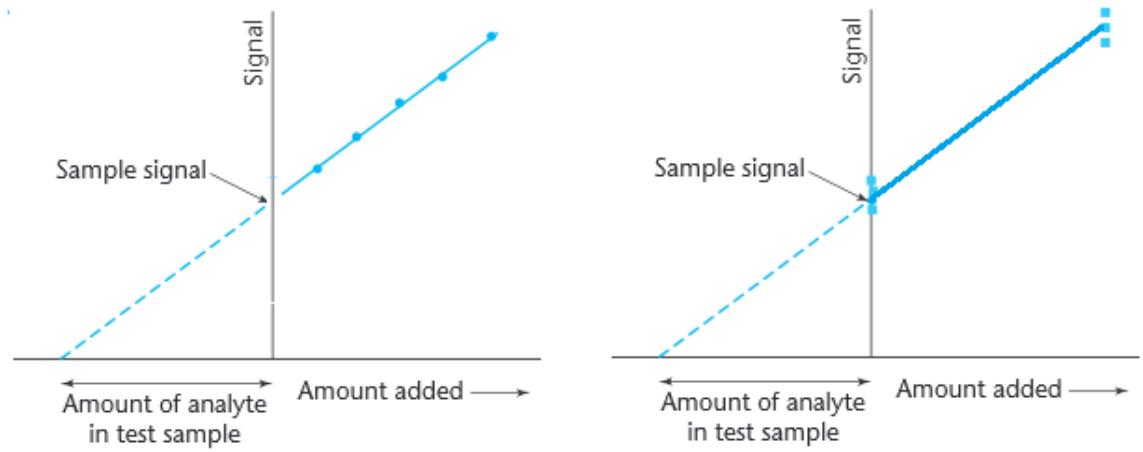

Figure 3.6 The estimation of the analyte concentration by the standard addition calibration. The curve on the left is plotted by preparing six separate calibration standards, and the curve on the right is plotted by performing three measurements on the original sample and three replicate measurements on a spiked sample containing a substantial amount of added analyte.

It is worth to be mentioned that the generated regression model must be linear over the studied range of added concentration, thus, the linearity was verified using the lack of fit method mentioned previously.

The formula for the standard deviation, S_{xE} of the extrapolated x-value (x_E) is given by the equation:

$$s_{x_E} = \frac{s_{y/x}}{b}\sqrt{\frac{1}{n} + \frac{\bar{y}^2}{b^2\sum_i (x_i - \bar{x})^2}} \qquad (3.8)$$

Where *b* is the slope, *n* is the number of observation and $S_{y/x}$ is the residual standard deviation. Thus, increasing the number of experiments reduce the extrapolated result imprecision, also winding the range of the analyte added concentration will increase the value $\sum_i (x_i - \bar{x})^2$ and reduce S_{xE}.

It is recommended to use six separate calibration standards (Figure 3.6, left), or perform three measurements on the original sample and three replicate measurements on a spiked sample containing a substantial amount of added analyte (Figure 3.6, right) [92]. However due to the lack of degrees of freedom, the latter approach was excluded. Moreover, due to the limitation of the salmon liver sample, it was decided to perform a total measurements of nine samples representing four experimental points (Figure 3.5).

3.2 Experimental

*3.2.1 Reagent*s

Prostaglandin E_2 (PGE_2, 99%), deuterated prostaglandin E_2 (PGE_2-d_4, 99%), leukotriene B_4 (LTB_4, 97%), deuterated leukotriene B_4 (LTB_4-d_4, 99%) were purchased from Cayman Chemical (Ann Arbor, MI, USA). Acetonitrile (liquid chromatographic grade, 99.8) was obtained from Sigma-Aldrich (St. Louis,MO, USA) and Chloroform (liquid chromatographic grade, 99.8%) was bought from Merck (Germany). Liquid nitrogen and dry ice were provided by Tess (Norway).

3.2.2 Samples preparation.

The initial concentrations of PGE_2, LTB_4, PGE_2-d_4, LTB_4-d_4 was 50 ng/ml, two stock solutions, designated as A and B, were prepared. Solution A containing 50 ng/ml of both PGE_2 and LTB_4 and solution B containing 50 ng/ml of both PGE_2-d_4 and LTB_4-d_4.

A wild salmon liver sample stored at -80°C was treated according to the above described extraction procedure (sub-section *2.2.2*).

Table 3.7 Concentrations of PGE_2, LTB_4, PGE_2-d_4 and LTB_4-d_4 in frozen liver sample at each experimental point of a two-variable Doehlert design

Experiment No.	Coded level		Natural level (ng/g)				Amount added from solution A µL	Amount added from solution B µL
	k_1	k_2	k_1		k_2			
			PGE_2	LTB_4	PGE_2-d_4	LTB_4-d_4		
1	0	0	25.00	25.00	32.5	32.5	150.0	195.0
2	0.5	-0.866	37.25	37.25	17.3	17.3	223.5	103.8
3	-0.5	0.866	13.20	13.20	47.7	47.7	79.20	286.2
4	-0.5	-0.866	13.20	13.20	17.3	17.3	79.20	103.8
5	0.5	0.866	37.25	37.25	47.7	47.7	223.5	286.2
6	-1.0	0	01.00	01.00	32.5	32.5	6.000	195.0
7	1.0	0	50.0	50.00	32.5	32.5	300.0	195.0
8*	NP	-0.866	00.00	00.00	17.3	17.3	00.00	130.8
9*	NP	0	00.00	00.00	32.5	32.5	00.00	195.0
10*	NP	0.866	00.00	00.00	47.7	47.7	00.00	286.2

*NP: Not present

Sample replication regime was corresponding to thr Figure 3.5

3.2.3 HPLC-MS/MS analysis

The LC/MS apparatus and the various instrumental and measurement conditions have been described above (section 2.2.3) however, the total analysis time was set to 20 min.

3.3 Results and discussion

The *RF* behavior for the COX metabolite (PGE_2 and PGE_2-d_4) and the LOX metabolites (LTB_4 and LTB_4-d_4) were modeled using a full-second order polynomial function with six coefficients (Eq. 3.4). Reduced models were also considered by ruling out less contributing coefficients. This was done when the adequacy and prediction capacity of the reduced model was not significantly affected in comparison with the six coefficients model. The fitness of the developed models was validated by comparing the ratio of experimental lack-of-fit to pure error variance at the determined degrees of freedom F_{cal} with F_{crit} as explained previously.
The variation of the analytes concentration between samples due to the differences in samples initial weight was considered (Appendix 1).

3.3.1 Modeling of the RF as a function of PGE_2 and PGE_2-d_4

The signal of the blank sample was initially subtracted from the experimental signals corresponding to the spiked samples dictated by the Doehlert design to eliminate the contribution of the endogenous level.
The experimental *RF* values at the various levels of concentrations of PGE_2 and PGE_2-d_4 were modeled successfully by using a six parameters regression models described by Eq. 3.4. This six parameters model was reduced to a four parameters model and expressed by:

$$RF = -4.61 + 0.0306 \times [PGE_2] + 0.014 \times [PGE_2\text{-}d_4] - 0.009 \times [PGE_2] \times [PGE_2\text{-}d_4] \quad (3.9)$$

The statistical acceptability of Eq. 3.9 was checked by means of a F-test as shown is Table 3.8. The *RF* variation as a function of PGE_2 in the range of 0 - 50 ng/g and PGE_2-d_4 in the range of 15-50 ng/g and according to Eq. 3.9 is presented in Figure 3.7.

The contour plot (figure 3.7) revealed that the *RF* remains constant in the whole range of PGE_2 when the internal standard is varied between (31.5 -32.5) ng/g.
Based on the *RF* behavior (Figure 3.7), a concentration of 31 ng/g of PGE_2-d_4 was selected as the optimal concentration of PGE_2-d_4 internal standard to analyze quantitatively PGE_2 in salmon liver.

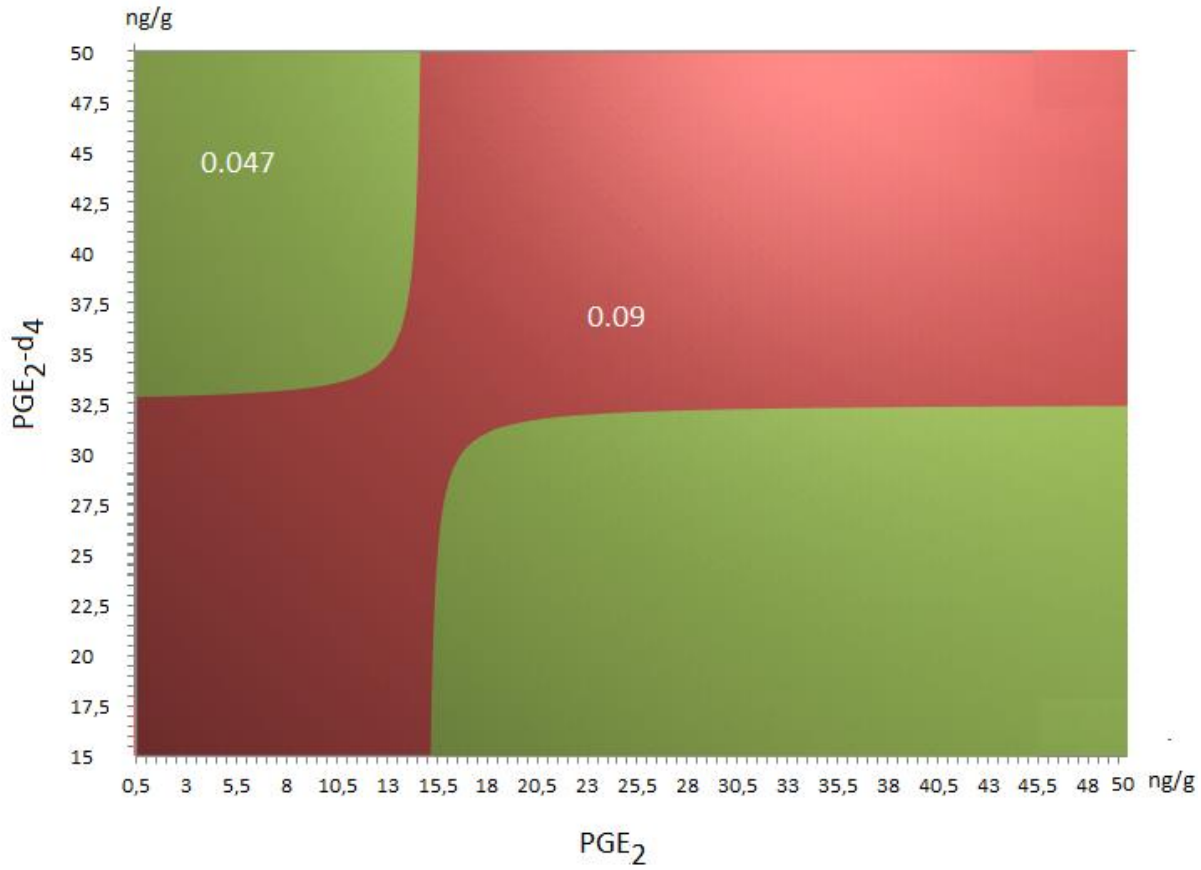

Figure 3.7 Contour plot of the response factor (*RF*) expressed as a function of PGE_2-d_4 vs. PGE_2

Table 3.8 Statistical validation results of the RF models for selecting optimal levels of internal standards associated with the analysis of LTB_4 and PGE_2 Salmon Liver.

	PGE_2	LTB_4
Residual Variance	12.46	0.23
Pure Error Variance	16.97	0.14
Lack Of Fit Variance	3.39	0.35
F calculated	0.199	2.49
F tabulated	3.700	3.700

3.2 Modeling of the RF as a function of LTB_4 and LTB_4-d_4

Similarly to the COX metabolite, the experimental *RF* values at the various levels of concentrations of LTB_4 and LTB_4-d_4 were modeled successfully, after subtracting the blank signals, by using a six parameters model of the form:

$$RF = -4.61 + 0.306\times [LTB_4] - 0.140\times [LTB_4\text{-}d_4] - 0.009\times [LTB_4]\,[LTB_4\text{-}d_4] \qquad (3.10)$$

The statistical acceptability of Eq. 3.9 was checked by means of a F-test as shown is Table 3.8. The model could not be reduced furtherly.

The *RF* contour plot generated by Eq. 3.10 as a function of LTB_4 and LTB_4-d_4 in the range of 0 - 50 ng/g and 15-50 ng/g respectively (Figure 3.8) displays three major regions, in which *RF* varied along LTB_4 axis, however, with the high concentration of LTB_4-d_4 (between 45-50 ng/g) the *RF* tends to be constant over the whole LTB_4 studied concentration range.

Based on the *RF* behavior (Figure 3.8) a concentration of 47.5 ng/g of LTB_4-d_4 was selected as the optimal concentration level of internal standard to analyze quantitatively LTB_4 in salmon liver.

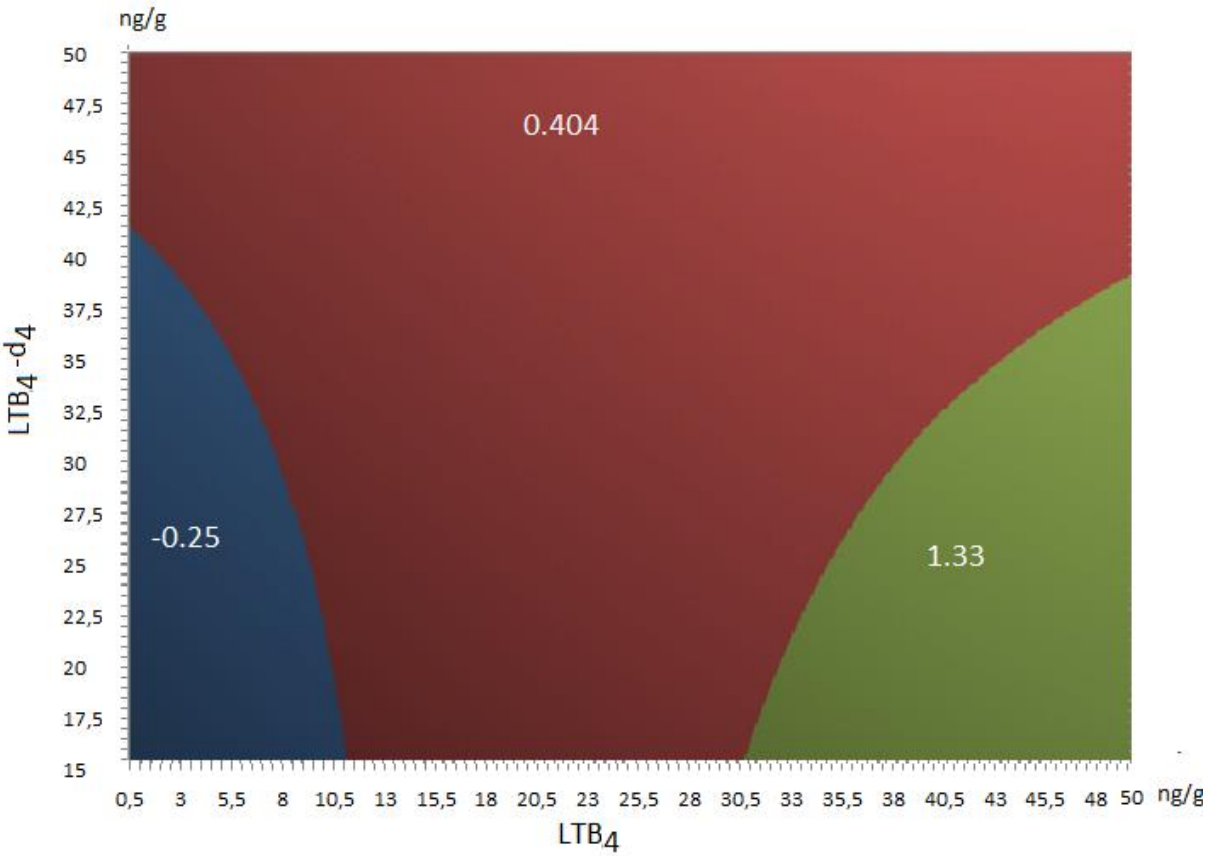

Figure 3.8 Contour plot of the response factor expressed as a function of LTB_4-d_4 vs. LTB_4.

3.3.3 Standard Addition Method to estimate the endogenous levels of eicosanoids

The quantification of endogenous levels of PGE_2 and LTB_4 were performed by the method of standard addition as follows. From the results of the previous Doelhert design (Table 3.5), calibration curves for PGE_2 and LTB_4 were generated and the concentration of the eicosanoids in the blank samples determined.

Each calibration curve was constructed from sets of four experimental points corresponding to three different levels of analyte (1, 25 and 50 ng/g) and one from the unspiked working samples. Each selected point contained constant amounts of PGE_2-d_4 and LTB_4-d_4 (32.5 ng/g) which were added to each sample.

Two samples were prepared for each point except the point that correspond to 25 ng/g of added analyte (the central point of the Doelhert design) of which three samples were prepared. The signal ratios PGE_2/PGE_2-d_4 and LTB_4/LTB_4-d_4 were plotted versus the concentrations of PGE_2 and LTB_4 respectively. Figure 3.9 shows the standards addition method regression curve for both PGE_2 and LTB_4.

The analyte endogenous concentration in the unspiked working samples was determined by extrapolating the calibration curve to the negative part of the concentration axis. Then, the absolute value of the x-intercept was calculated to estimate the amount of PGE_2 and LTB_4 in the unspiked blank salmon liver. The results in Table 3.9 showed that the endogenous levels were found 101.46 ±48.48 ng/g and 86.67±41.28 ng/g with the confidence level of 95% for both PGE_2 and LTB_4 respectively.

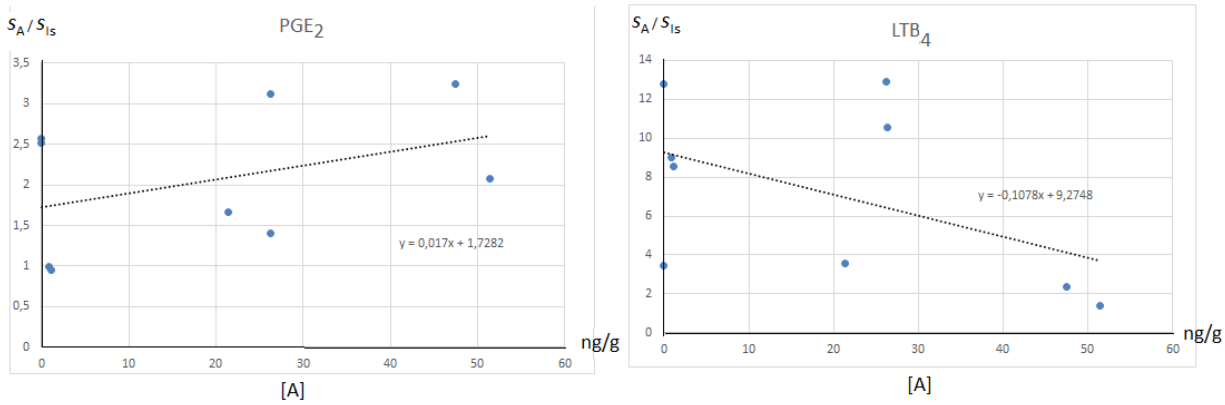

Figure 3.9 standards addition method regression curve for both PGE_2 and LTB_4 Where [A] is the analyte concentration and S_A/S_{IS} in the signal of the analyte to the signal of the internal standard ration.

Table 3.9 Quantification of PGE_2 and LTB_4 in working sample using the standard addition method

	PGE_2	LTB_4
Standard addition Calibration line slop	0.017	-0.108
Standard addition Calibration line intercept	1.73	9.27
Endogenous concentration ng/g	101.46	86.67
RSD%	16.28	16.44

Figure 3.9 shows that generated the linear regression curve that correspond to LTB_4 had a negative slop, this could be due to the major variation of the response factor, as shown in Figure 3.8., when using the concentration of 32.5 ng/g of internal standard.

Also, the LTB_4 production might differ within the same liver, depending on which type of liver cells the samples contain the most. For instance LTB_4 are produced in both hepatocyte and kupffer cells but not in the endothelial cells [5], these points might have affected the sensitivity of the test and caused a negative slop, however, suggestion regarding the method improvement and sample homogenization are given in section 4.8.

3.3.4 Remodeling of the RF as a function of PGE_2 and PGE_2-d_4 by considering the contribution of the endogenous levels (101 ng/g) in the blank salmon liver

By considering the endogenous level of 87 ng/g, the analytical range of 87-137 ng/g was estimated and the behaviors of the *RF* was studied as explained above (section 3.3.1). The results indicated that the suggested model was found as follows:

$$RF = -7.26 + 0.074 \times [PGE_2] + 0.38 \times [PGE_2\text{-}d_4] - 0.003 \times [PGE_2] \times [PGE_2\text{-}d_4] \quad (3.11)$$

The suggested model was validated by the mean of F-test as mentioned in table 3.10.

The RF behavior over the studied range is represented in the Figure 3.10, The *RF* tends to be constant when the level of internal standard varied between (20-31) ng/g

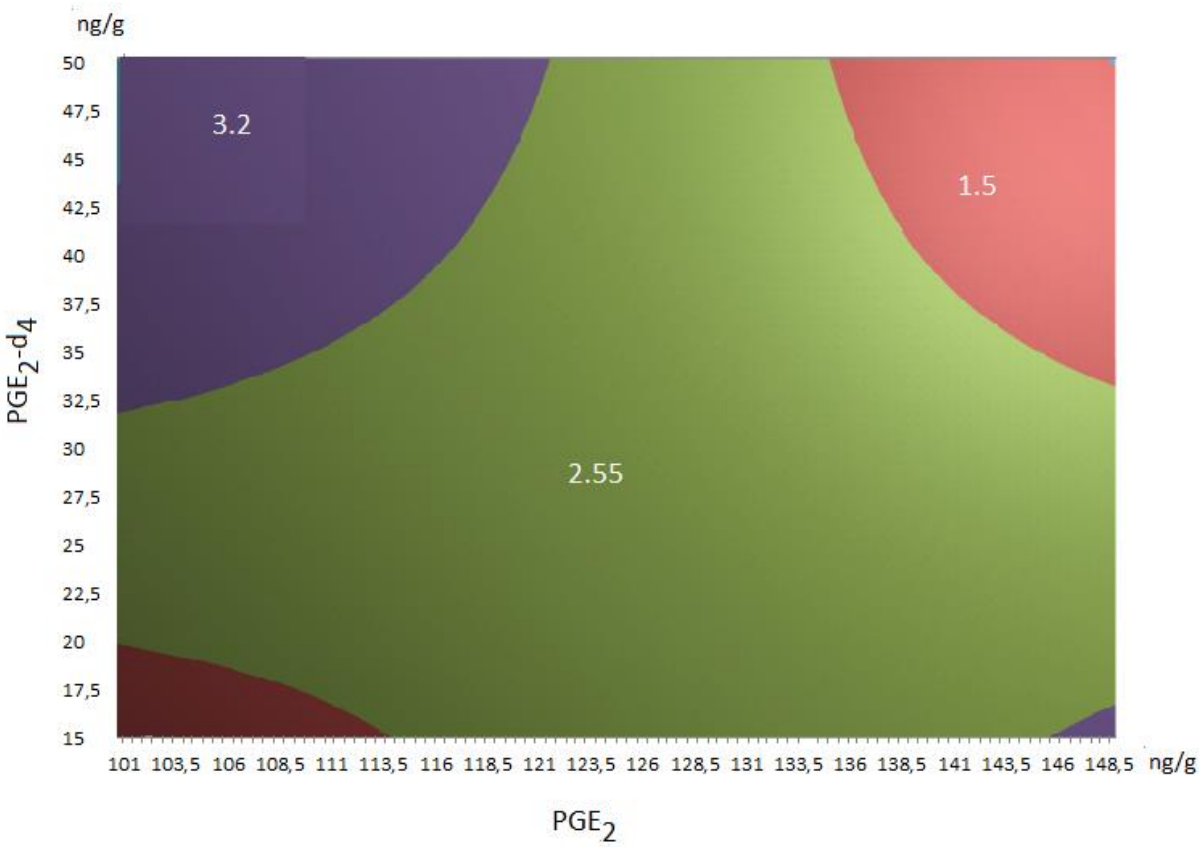

Figure 3.10 Contour plot of the response factor (*RF*) expressed as a function of PGE_2-d_4 vs. PGE_2 After considering the endogenous level of LTB_4.

3.3.5 Remodeling of the RF as a function of LTB_4 and LTB_4-d_4 by considering the contribution of the endogenous levels (87 ng/g) in the blank salmon liver

By considering the endogenous level of 87 ng/g, the analytical range of 87-137 ng/g was estimated and the behaviors of the *RF* was studied as explained above (section 3.3.2). The results indicated that the suggested model was found as follows:

$$RF = -6.85 + 0.1\times [LTB_4] - 0.04\times [LTB_4\text{-}d_4] - 0.002\times [LTB_4]\,[LTB_4\text{-}d_4] + 0.0022\,[LTB_4\text{-}d_4]^2 \quad (3.12)$$

The statistical acceptability was checked by F-test. Table 3.10.

The *RF* was studied over the whole range using the equation 3.12, and plotted in Figure 3.11, the *RF* tends to be constant when the concertation of internal standard was set to be 50 ng/g.

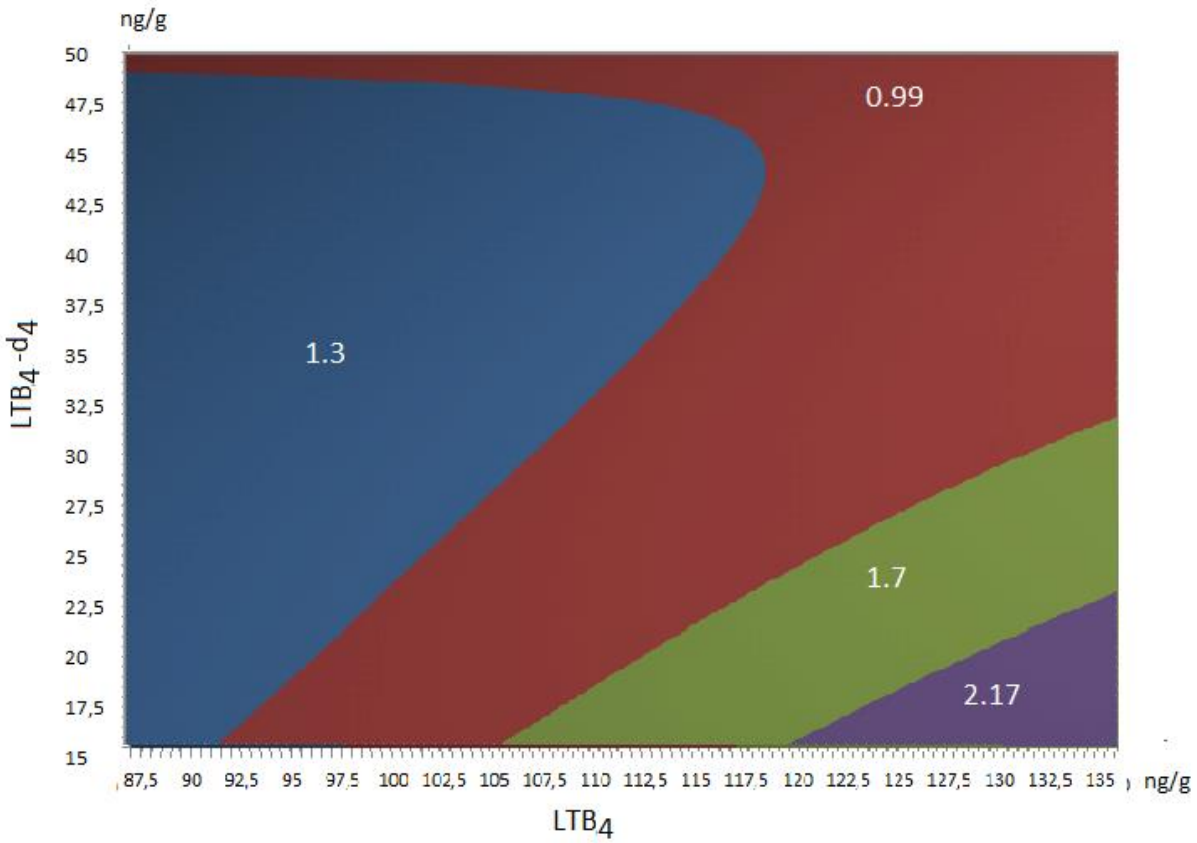

Figure 3.11 Contour plot of the response factor expressed as a function of LTB_4-d_4 vs. LTB_4 After considering the endogenous level of LTB_4

In order to assess the variability of the RF over the studied range on analyte concentration, another approach was used:

Using both equations 3.11 and 3.12, the *RF* was calculated along the whole studied range of 87- 101-151 ng/g and 137 ng/g for both PGE_2 and LTB_4 respectively and the range of 15 – 50 ng/g regarding both PGE_2-d_4 and LTB_4-d_4. And the variability of *RF* PGE_2 and *RF* LTB_4, expressed as relative standard deviation (RSD) was studied (Fig.3.12).

The RSD increased in the whole range of PGE_2 as the concentration of PGE_2-d_4 increased in the range of 15–50 ng/g. While the RSD decreased in the whole range of LTB_4 as the concentration of LTB_4-d_4 increased in the range of 15–50 ng/g.

On average, it was estimated that the optimal concentrations of PGE_2-d_4 and LTB_4-d_4 yielding constant *RF* PGE_2 and *RF* LTB_4, in the whole range of PGE_2 and LTB_4 and with the minimum dispersion, lies between 25-30 ng/g and 45-50 ng/g respectively.

The optimal selected concentration was 25 ng/g and 50 ng/g for both of PGE_2-d_4 and LTB_4-d_4 respectively.

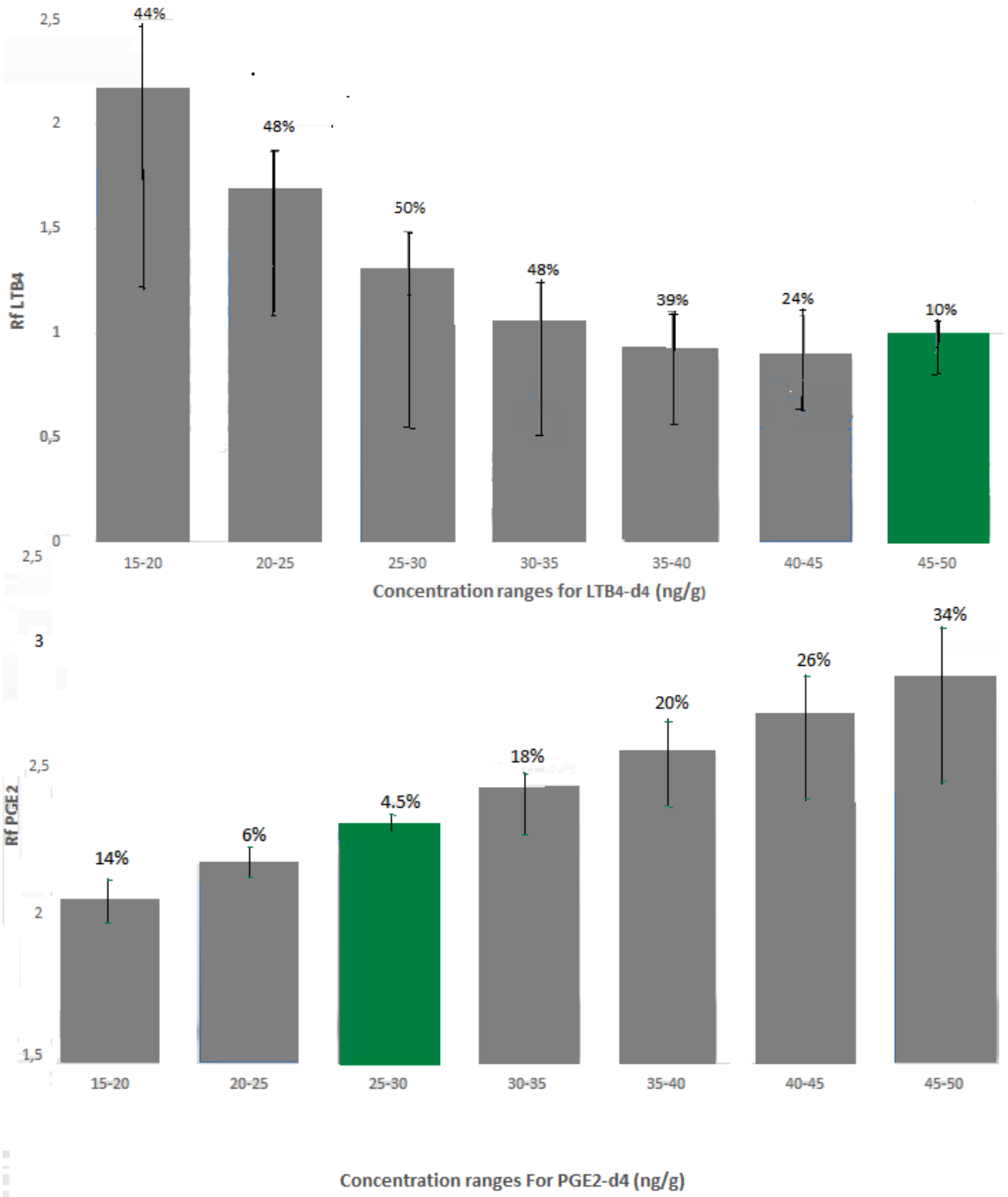

Figure 3.12 Average PGE_2 and LTB_4 response factors (*RF* PGE_2 and *RF* LTB_4) and associated relative standard deviations (RSD%) at different concentration ranges of PGE_2-d_4 and LTB_4-d_4. The green bars represent optimal concentrations of internal standards (in ng/ml) yielding constant *RF* and minimum RSD in the whole range of analytical concentrations.

Table 4.1 PGE_2 and LTB_4 calibration curves regression coefficients and statistical validation results for the obtained model.

	PGE_2	LTB_4
Correlation Coefficient	0.40	0.48
Variance of residual error (VRE)	0.71	0.18
Variance of pure error (VPE)	0.48	60.20
Variance of lack of fit (VLOF)	0.62	0.85
Calculated F (Fcal)	1.30	0.96
Tabulated F (F tab)	5.78	5.78

3.4 Conclusions

The two-factor Doehlert uniform shell design demonstrated to be an efficient strategy to estimate rationally and comprehensively the optimal levels of internal standards, specifically PGE_2-d_4 and LTB_4-d_4, in addition to the analytical range for PGE_2 and LTB_4 where is expected a linear behavior.

The optimal concentration was found 25 ng/g and 50 ng/g for both of PGE_2-d_4 and LTB_4-d_4 respectively.

Standard addition method was performed to estimate the endogenous level of eicosanoids in the working sample, the endogenous level was found 101.46 ±48.48 ng/g and 86.67±41.28 ng/g with the confidence level of 95% for both PGE_2 and LTB_4 respectively.

.

4. Method Validation

Method validation is the confirmation of the method precision and reliability by defining the characteristic of the method to guarantee that the procedure, when correctly applied, produces results that are fit for purpose [1, 82].

After the selection of the optimal internal standard concentrations, the developed LE-HPLC-MS/MS method was submitted to analytical validation. The considered validation parameters were: selectivity, limit of detection, limit of quantification, linearity, analytical range, precision recovery and stability.

4.1 Selectivity

Selectivity of a method is defined by the ability of the method to determine a particular analyte in a complex mixture without interference from other components in the mixture [95].
In chromatographic techniques compounds are separated and eluted in different retention times which can guarantee the selectivity, the selectivity is assessed by the terms Resolution (Rs) which is defined by the equation:

$$\mathrm{Rs} = \frac{\Delta t}{\frac{1}{2}(W_A - W_B)} \qquad (4.1)$$

While Δt is the separation time difference between two peaks and W is chromatographic peak width at base [1, 95].
When the chromatographic method is coupled with mass spectroscopy, the mass spectra guarantee more selectivity [96].
In this thesis the selectivity was assessed by evaluating the extracted ion chromatogram EIC of PGE_2, LTB_4, LTB_4 –d_4 and PGE_2 - d_4. As shown in Figure 4.1, the method was highly selective, this selectivity allows the use of isotopically labelled analytes as internal standards, and distinguish between the obtained signals.

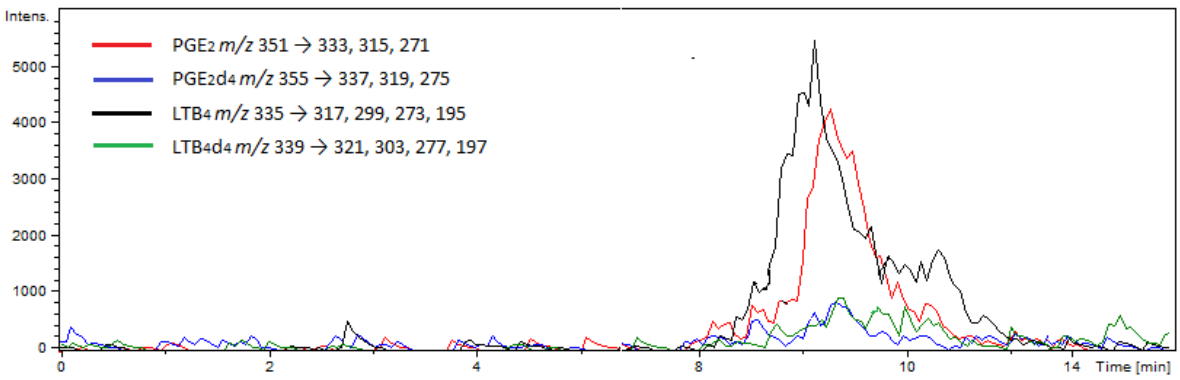

Figure 4.1 EIC of PGE2, LTB_4, LTB_4 –d_4 and PGE_2 -d_4 spiked in a wild salmon liver sample.

4.2 Linearity

Linearity is the ability of an analytical method to provide an analytical response proportional to the concentration or the amount of analyte within a specified range of analyte concentration [83].

Linearity is expressed by the linear regression equation:

$$y = a\,(x) + b \qquad (4.2)$$

Where *y*, in the present study, is the analyte/internal standard signal ratio, *x* is the analyte concentration and *a* and *b* are the slope an intercept of the calibration function respectively.

In common practice the linearity of a calibration curve is assessed by calculating the correlation coefficient (r) [95].

$$r = \frac{n\sum x_i y_i - \sum x_i \sum y_i}{\sqrt{[n\sum x_i^2 - (\sum xi)^2][n\sum y_i^2 - (\sum y_i)^2]}} \qquad (4.3)$$

A correlation coefficient close to unity (r = 1) is traditionally considered sufficient evidence to conclude that the experiment has a perfect linear calibration. However, the correlation coefficient close to one does not necessarily imply the linearity of a regression model. Moreover, the linearity must be checked using the F-test previously described in the section 3.1.6.

The developed method was assessed by using Eq. 4.2 in the range of 1-50 ng/g of PGE_2 and LTB_4 and the linearity of the model for both analytes assessed by the F-test as indicated in Table 4.1.

Table 4.1 PGE_2 and LTB_4 calibration curves regression coefficients and statistical validation results for the obtained model.

	PGE_2	LTB_4
Slop a	0.017	-0.107
Intercept b	1.720	9.274
Correlation Coefficient	0.402	0.484
Variance of residual error (VRE)	0.710	0.180
Variance of pure error (VPE)	0.480	0.600
Variance of lack of fit (VLOF)	0.620	0.850
Calculated F (Fcal)	1.300	0.960
Tabulated F (F tab)	5.780	5.780

4.3 Precision

Precision is defined as the closeness of agreement between a quantity values obtained by series of replicate measurements of the same quantity under the prescribed conditions [95]. Repeatability, intermediate precision and reproducibility are three terms associated with precision [1].

Repeatability is the precision of results obtained in the same measurement conditions (global factors) such as analyst, preparation, laboratory, instrument, etc. over a short period of time while the intermediate precision is the precision of results obtained in a given laboratory over an extended period of time [1].

Reproducibility is the precision of results obtained by changing one or more global factors over a short or an extended period of time.

It is expressed by the standard deviation (SD), variance (SD^2), relative standard variation (RSD) or coefficient of variation (CV) of replicate measurements and given by the following equations:

$$SD = \sqrt[2]{\frac{\sum_{i=0}^{n} (x_i - \bar{x})^2}{n-1}} \quad (4.4)$$

$$RSD = \frac{SD}{\bar{x}} \quad (4.5)$$

$$CV = \frac{SD}{\bar{x}} \times 100 \quad (4.6)$$

Where $\bar{x}$ is the mean value, *n* is number of measurements and *n-1* is the degrees of freedom [83].

4.4 Accuracy

Accuracy is the degree of agreement between the experimental value, obtained by replicate measurements, and the accepted reference value [83].

Among different strategies to estimate the accuracy of a method, the terms recovery was used as a numerical value to assess accuracy in this thesis, this was mainly because a blank sample of salmon liver was not available as nor was certified reference material.

The recovery, expressed in percentage units (%), of an analytical method for a given analyte in a certain biological sample is calculated by using the general formula:

$$Rec = \frac{C_m}{C_+} \times 100 \quad (4.7)$$

Where Rec is recovery, C_m is the analyte concentration measured by the analytical method in the biological sample, and C_+ is the known nominal concentration of the analyte added to the sample [97].

However, when the analyte naturally exists in the biological sample at a basal concentration level (endogenous level) $C_{0,Ln}$ this concentration must be considered and subtracted from the measured concentration C_m, when calculating the methods recovery for the analyte for each added concentration [97]

Thus, the recovery of endogenous substances in their biological matrices is calculated using the formulas:

$$\text{Rec} = \frac{Cm - C_{0\,Ln}}{C_{+}} \times 100 \qquad (4.8)$$

In this thesis, the precision and accuracy was estimated from Doelhert design experiments by calculating the coefficient of variation and recovery obtained from duplicate spiked liver samples with low and high levels of PGE_2 and LTB_4 (1, and 50 ng/g respectively) and triplicate samples spiked with medium concentration level (25 ng/g) measurements. All samples were spiked with constant level of PGE_2-d_4 and LTB_4-d_4 (32.5 ng/g) and the results are shown in Table 4.2.

4.5 Limit of detection (LOD) and limit of quantification (LOQ)

The LOD is the lowest concentration or amount of an analyte in a sample that can be detected, but not necessarily quantified whereas the LOQ is the lowest concentration of an analyte in a sample that can be determined with acceptable level of confidence [95].

LOQ and LOD are usually calculated from at least six blank analysis results, the LOD is defined as the analyte concentration corresponding to the sample blank value plus three standard deviation and LOQ is the analyte concentration corresponding to the sample blank value plus 10 standard deviations [83].

$$\text{LOD} = \bar{X} + 3\,SD_{blank} \qquad (4.9)$$

$$\text{LOQ} = \bar{X} + 10\,SD_{blank} \qquad (4.10)$$

$$\text{LOQ} = 3.3\ \text{LOD} \qquad (4.11)$$

Where $\bar{X}$ is the average of concentration estimation of the blank (usually zero) and SD_{blank}. Therefore, both LOD and LOQ have experimentally measured values and require the availability of a blank sample. However, in the case of this study a blank sample was not available.

It was suggested that the actual LOQ of a method for endogenous substances is the lowest added analyte concentration, C_{LOQ}, to the biological sample that can be measured with acceptable

accuracy (Rec %) and precision (CV) and that can be discriminated statistically significantly from the basal concentration $C_{0,Ln}$ of the analyte in relevant biological sample [96].

Furthermore, an additional performance parameter has been suggested, The relative limit of quantification, rLOQ, as the ratio of the lowest added analyte concentration C_{low+} to the basal natural concentration $C_{0,Ln}$, and calculated from the equation:

$$\text{rLOQ} = \frac{C_{\text{LOQ}}}{C_{0,\text{Ln}}} \times 100 \qquad (4.12)$$

The rLOQ expresses the percentage fraction of the analyte which, upon addition to the biological sample that contains this analyte in the basal concentration $C_{0,Ln}$, can be measured therein with acceptable accuracy [97].

Furthermore, it was proposed that LOQ and rLOQ be corrected, by the recovery values with which the LOQ values have been determined experimentally to become the recovery-corrected, LOQ, LOQ_{Rec}:

$$\text{LOQ}_{\text{Rec}} = \frac{\text{rLOQ}}{Rec@C_{\text{LOQ}}} \qquad (4.13)$$

Whereas $\text{Rec@C}_{\text{LOQ}}$ is the value of recovery with which the C_{LOQ} is determined [97].

4.6 Range

The range of an analytical method is defined as the interval between 2 concentration of analyte for which suitable precision, accuracy and linearity have been demonstrated. Thus, it is possible to differentiate between two types of range; working (analytical) range and linear (calibration) range.

Analytical range describes the interval between the LOD and the highest concentration where the signal can be related to the concentration for the evaluation of random and systematic errors. The linear range corresponds to the valid functional interval where the dependence of the signal on concentration validated using the method of least square [95].

In this thesis, LOD could not be defined since a blank sample was not available, and the linear dependence of the analyte signal on the concentration over the studied range (in Doelhert design experiments) was validated using the F-test, the reader is referred to section 3.1.6.

Table 4.2 shows the method linear range regarding both PGE_2 and LTB_4.

Table 4.2 The validation parameters at each calibration points

Analyte	Endogenous concentration (ng/g)	Calibration point number	Number of replicates	Concentration after analyte addition (ng/g)	Concentration estimated (ng/g)	Precision CV %	Accuracy Rec %	Rang ng/g
PGE2	101.64	1	2	102.5	26.4	74	- 9181	1-50
		2	3	126	12	52	- 302	101-151
		3	2	151	33.5	26	-136	
LTB4	86.67	1	2	88	258	10.5	701	1-50
		2	3	111	238	60	15650	87 - 134
		3	2	136	52	30	-69	

It has been suggested for analytical methods, when determining the amount of an analyte in a biological sample, that the acceptable accuracy (recovery%) is 100±20% and precision (CV) ≤20% [96.97]. Based on this, neither recovery nor precision values shown in table 4.2 are acceptable. Therefore rLOQ was not calculated. This might be because the concentration of IS used was 32.3 ng/g, which is not the optimum concentration for the quantification of LTB_4 and PGE_2. However, an optimum concentration of TLB_4-d_4 was used in two experimental points in the Doelhert design while unfortunately the optimum concentration of PGE_2-d_4 was never used in any experimental point since the only the Doelhert experimental were carried out, more experiments using the optimum concentration of internal standard need to carried out, unfortunately, time and salmon liver sample limitations did not allow preforming more experiments.

Table 4.3 shows the validation parameters for the quantification of LTB_4 when samples were spiked with 47.7 ng/g of internal standard.

Table 4.3. The validation parameters when the optimum concentration of LTB_4-d_4 was added to samples

Endogenous concentration (g/g)	Number of replicates	Concentration after analyte addition (ng/g)	Concentration estimated (ng/g)	Precision CV %	Accuracy Rec %	rLOQ %	rLOQRec %
86.67	2	98.9	97.42	20.6	98.4	15.5	16.7
	3	127.05	132.23	19.06	104	-	-

4.7 Stability

A loss in the target analyte might occur during the sample processing and storage, this might be because of different reasons (e.g. chemical degradation, adsorption on the test tube, etc.), thus, the stability of the analyte in solvent and sample extracts should be assessed [99].

The stability of PGE_2 and LTB_4 in the sample extract was assessed by storing samples extract in room temperature (+20 C°), fridge (+4 C°), and freezer (-80 C°), the samples were injected in the LC-MS for 3 consecutive days and the intensity of the target analytes compared to the intensity at day zero.

Samples extracts were prepared from the same liver with the same procedure mentioned in section 3.2.2, and kept in disposable plastic tubes during storage.

Before the injection samples were vacuum dried, diluted to 40 µL with acetonitrile then centrifuged at 6037×g for 1 min then injected in the LC-MS. Table 4.4 shows the relative target analyte EIC peak area obtained by MS in different days in samples stored in different conditions compared to the peak area of target analytes obtained by injecting the sample on the same day of preparation.

Table 4.4 Relative EIC peak areas for target analytes stored in different temperature over three days.

	Storing temperature C°	Relative peak area PGE_2 %	Relative peak area LTB_4 %
Day 1	-80	123	97
	+4	108	65
	+20	122	73
Day 2	-80	188	97
	+4	113	63
	+20	107	93
Day 3	-80	168	83
	+4	317	158
	+20	180	76

It was noticed from Table 4.4 that there was no significant change in the MS signal for neither PGE_2 and LTB_4 after one day of storage in the -80 °C. However, it was clear that the LTB_4 signal has decreased in the second and third storing day regardless of the storage temperature while the signal of PGE_2 increased.

The increase of the PGE_2 signal could be explained by the formation of PGD_2, PGD_2 is known to be a stable isomer of PGE_2. Also, PGD_2 MS fragmentation products were reported to have similar m/z to those of PGE_2 MS fragmentation [99], PGE_2 formation might be caused by PGE_2 degradation.

4.8 Conclusions and suggestions for further work

The developed method exhibited good selectivity, linearity over the range (1-50) ng/g for both PGE_2 and LTB_4 respectively. In addition, the endogenous levels for PGE_2 (87 ng/g) and LTB_4 (101 ng/g) indicate that the system linearity could be extended until 137 ng/g and 151 ng/g respectively.

The method precision for LTB_4 quantification was found 19-20.6% and the recovery ranged between 98.4-104%, the relative limit of quantification rLOQ was found 15.5%.

Both PGE_2 and LTB_4 were found stable at -80 °C for 24 hour after the extraction.

In the present thesis the amount of available wild salmon liver was limited. For that reason, portion of the same liver were cut and processed for different kind of experiments. For example, the portions of liver were separated and submitted to the simplex design optimization, the Doehlert experiments and the stability studies. It was reported that eicosanoids endogenous levels might differ within the same liver, hepatocyte produce a small amount of PGE_2 comparing to both kupffer and endothelial cells [5]. Consequently, it is important to submit the whole liver to the pulverization procedure proposed in the present thesis to ensure a high degree of sample homogeneity and a more uniform distribution of eicosanoids in the blank samples.

Adding small glass pellets equivalent to the sample size (~0.3 g) to process the liver samples and using ultra sound water bath could improve the extraction of the analytical species. This suggestion was assessed by adding a volume of glass pellets and submitting the system to ultrasound after adding the extraction solvents. The final results revealed a clear and bright yellow oil system (Figure 4.2 A) that was not furtherly processed due to time restriction.

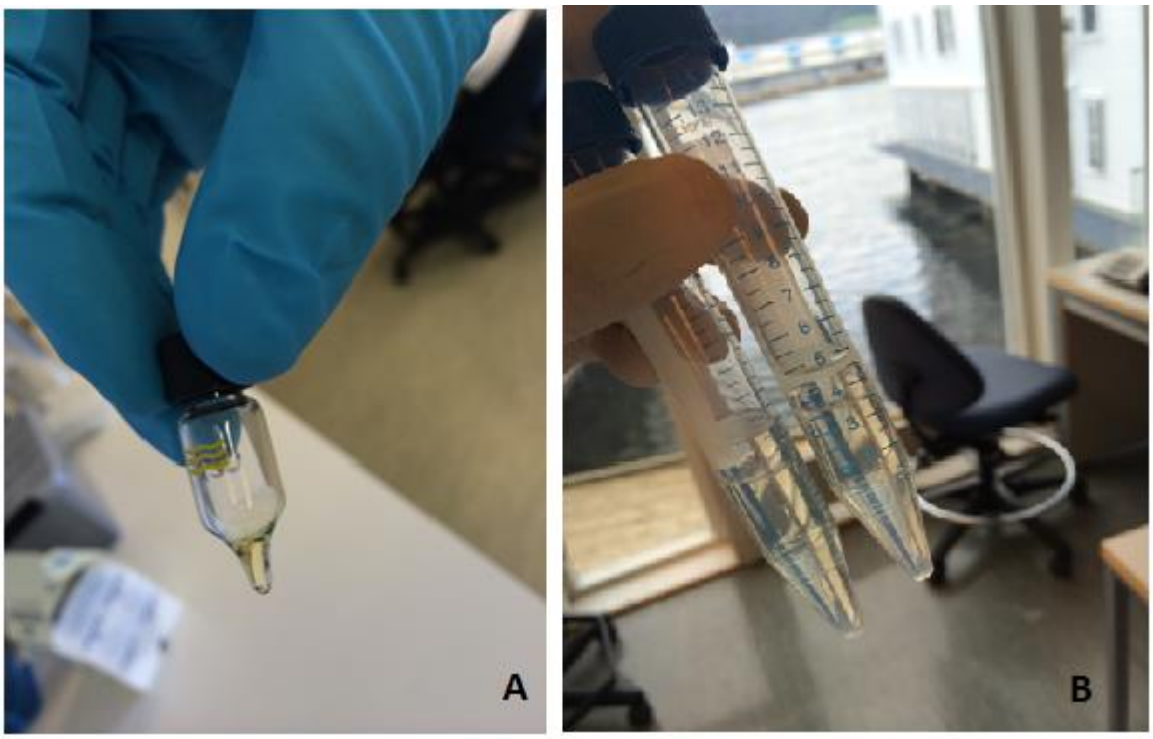

Figure 4.2 A. The oily phase remained after evaporating the extract, it was not able to inject in the LC/MS instrument. B. the extract after adding the (1:1) hexane methanol solution, the fatty phase was dissolved in the hexane phase.

Perhaps, it would be advisable to add a mixture of methanol :hexane to separate the non polar components (Figure 4.2B).

The concentration range of the internal standard proposed to be optimized was (15-50) ng/g, however, after considering the endogenous level of the analyte in the blank sample the range of the analyte concentration investigated was expanded to 150 ng/g and 137 ng/g for both PGE_2 and LTB_4 respectively, thus the range of the internal standard should be extended to be between (75-125) ng/g, also method validation should be performed using the exact optimal amount of the internal standard.

6. References

[1] Y. Yang. Development of a solid phase extraction method for evaluating the production of classic and nonclassic eicosanoids inhuman and fish cells using liquid chromatography tandem mass spectrometry, *Master Thesis, UiB publication*. **2014**.

[2] P. Calder. Long-chain polyunsaturated fatty acids and inflammation. *Scandinavian Journal of Food and Nutrition.* **2006**, *50*, 54 -61.

[3] M. Hamilton, R. Hites, S. Schwager. Lipid composition and contaminants in farmed and wild salmon. *Environmental Science and Technology.* **2005**, *39*, 8622-8629.

[4] Gomes, E. Fernandes, A. Silva, C. Santos, D. Pinto. Anti-inflammatory potential of 2-styrylchromones regarding their interference with arachidonic acid metabolic pathways. *Biochemical Pharmacology*. Elsevier, **2009**, *2*, 171-78.

[5] K. Tolman. Eicosanoids and the liver. *Prostaglandins & other Lipid Mediators*.**2000**, *61*, 163–174.

[6] S. Lundström, F. D'Alexandri, K. Nithipatikom, J. Haeggström. HPLC/MS/MS-Based approaches for detection and quantification of eicosanoids. *Lipidomics, Methods in Molecular Biology.* **2009**, 579, 161-187.

[7] L. Kortza, J. Dorowa and U. Ceglareka. Liquid chromatography–tandem mass spectrometry for the analysis of eicosanoids and related lipids in human biological matrices: A review. *Journal of Chromatography B.* **2014**, *964*, 1–11.

[8] P. yang C. Cartwright, J. LI, S. Wen. Arachidonic acid metabolism in human prostate cancer. *International journal of oncology*. **2012**, *41*, 1495-1503.

[9] Teo, W. Chong, E. Tan, N. Basri, Z. Low. Advances in sample preparation and analytical techniques for lipidomics study of clinical samples. *Trends in Analytical Chemistry.* **2015**, *65*, 1–18.

[10] H.Minamisawa, A.Terashi, Y. Katayama, Y. Kanda, Jun Shimizu, T.Shiratori, K.Inamura, H. Kaseki, Y. Yoshino. Brain eicosanoid levels in spontaneously hypertensive rats after ischemia with reperfusion: Leukotriene C4 as a possible cause of cerebral edema. *Stroke* **1988**. *19*, 372-377.

[11] Y. Cao, C. Zhou, L. Sun, R.Xue, J. Xu and Z. Liu: Chronic administration of ethyl docosahexaenoate reduces gerbil brain eicosanoid productions following ischemia and reperfusion. *Journal of Nutritional Biochemistry.* **2006**, *17*, 234–241.

[12] T. Ogorochi, S. Narumiya, N. Mizuno, K. Yamashita, H. Miyazaki, O. Hayaishi, Regional distribution of prostaglandins D2, E2, and F2α and related enzymes in postmortem human brain. *Journal of Neurochemistry*. **1984**, *43*, 71–8.

[13] M. Abdel-Halim, B. Sjöquist, E. Änggård, Inhibition of prostaglandin synthesis in rat brain. *Acta Pharmacology and Toxicology*.**1978**, *43*, 266–272.

[14] S. Amruthesh, J. Falck, E. Ellis. Brain synthesis and cerebrovascular action of epoxygenase metabolites of Arachidonic Acid. *Journal of Neuro chemistry*. **1992**, *58*, 503–510.

[15] Wiswedel, D. Hirsch, J. Nourooz-Zadeh, A. Flechsig, A. Lück-Lambrecht and W. Augustin, Analysis of Mono hydroxyl eicosatetraenoic Acids and F2 -isoprostanes as Markers of Lipid Peroxidation in Rat Brain. Mitochondria Free Radical. **2002**, *36*, 1–11.

[16] Milatovic, M. Aschner, Measurement of Isoprostanes as Markers of Oxidative Stress in Neuronal Tissue. *Current Protocol Toxicology*. **2009**, 12–14.

[17] S. Yang, Y. Ma, Y. Liu, H. Que, C. Zhu, S. Liu. A Bridge between Traumatic Brain Injury and Fracture Healing Neurotrauma. *Journal of Arachidonic Acid.* **2002**, *29*, 2696–2705.

[18] S.K. Abbott, A.M. Jenner, T.W. Mitchell, S.H. Brown, G.M. Halliday, B. Garner. An improved high-throughput lipid extraction method for the analysis of human brain lipids. *Lipids.* **2013**, *48*, 307–318.

[19] R. Saunders, L. Horrocks. Simultaneous extraction and preparation for high-performance liquid chromatography of prostaglandins and phospholipids. *Analytical Biorchemistry*.**1984**, *143*, 71–75.

[20] Birkle, H. Bazan, N. Bazan. Analysis of prostaglandins, leukotrienes, and-related compounds in retina and brain. *Lipids and Related Compounds*. **1989**, 227–244.

[21] Y. Yasaka, M. Tanaka, T. Shono, T. Tetsumi, and J.I. Katakawa, 2-(2,3-Naphthalimino) ethyl trifluoro methane sulphonate as a highly reactive ultraviolet and fluorescent labelling agent for the liquid chromatographic determination of carboxylic acids. *Chromatography A*. **1990**, *508*, 133–140.

[22] H. Yue, K.I. Strauss, M.R. Borenstein, M.F. Barbe, L.J. Rossi, and S.A. Jansen, Determination of bioactive eicosanoids in brain tissue by a sensitive reversed-phase liquid chromatographic method with fluorescence detection. *Chromatography. B*. **2004**, *803*, 267–277.

[23] J.A. Yergey, H.Y. Kim, and N. Salem Jr., High-performance liquid chromatography/thermospray mass spectrometry of eicosanoids and novel oxygenated metabolites of docosahexaenoic acid. *Analytical Chemistry.* **1986**, *85*, 1344-134.

[24] M. Masoodi, and A. Nicolaou, Lipidomic analysis of twenty-seven prostanoids and isoprostanes by liquid chromatography/electrospray tandem mass spectrometry. *Rapid commune Mass Spectrometry*. **2006**, *20*, 3023–302.

[25] H. Yue, S.A. Jansen, K.I. Strauss, M.R. Borenstein, M.F. Barbe, L.J. Rossi, and E. Murphy. A liquid chromatography/mass spectrometric method for simultaneous analysis of arachidonic acid and its endogenous eicosanoid metabolites prostaglandins, dihydroxyeicosatrienoic acids, hydroxyeicosatetraenoic acids, and epoxyeicosatrienoic acids in rat brain tissue. *Pharmceutic Biomedicine Analysis*. **2007**, *43*, 1122–1134

[26] M. Masoodi, A. Mir, N.A. Petasis, C.N. Serhan, and A. Nicolaou. Simultaneous lipidomic analysis of three families of bioactive lipid mediators leukotrienes, resolvins, protectins and related hydroxy-fatty acids by liquid chromatography/electrospray ionization tandem mass spectrometry. *Rapid commune Mass Spectrometry*. **2008**, *22*, 75–83.

[27] M.Y. Golovko, and E.J. Murphy. An improved LC-MS/MS procedure for brain prostanoid analysis using brain fixation with head-focused microwave irradiation and liquid-liquid extraction. *Journal of Lipids*. **2008**, *49*, 893–902.

[28] S.E. Farias, M. Basselin, L. Chang, K.A. Heidenreich, S.I. Rapoport, and R.C. Murphy. Formation of eicosanoids, E_2/D_2 isoprostanes, and docosanoids following decapitation-induced ischemia, measured in high-energy-microwaved rat brain *Journal of Lipids*. **2008**, 49, 1990–2000.

[29] S.A. Brose, B.T. Thuen, M.Y. Golovko. LC/MS/MS method for analysis of E_2 series prostaglandins and isoprostanes. *Journal of Lipids*. **2011**, *52*, 850–859.

[30] D.S. Dumlao, M.W. Buczynski, P.C. Norris, R. Harkewicz, E.A. Dennis. High-throughput lipidomic analysis of fatty acid derived eicosanoids and N-acylethanolamines. *Lipids.* **2011**, *1811*, 350-362.

[31] D. Nomura, B. Morrison, J. Blankman, J. Long, S. Kinsey, M. Marcondes, A. Ward, Y. Hahn, A. Lichtman, Endocannabinoid Hydrolysis Generates Brain Prostaglandins That Promote Neuro inflammation. *Science*, **2011**, *334*, 809-813.

[32] G. Unterwurzacher, T. Koal, G. K. Bonn, K. M. Weinberger and S. L. Ramsay. Rapid sample preparation and simultaneous quantitation of prostaglandins and lipoxygenase

derived fatty acid by liquid chromatography-mass spectrometry from small sample volumes. *Clinical Chemistry Laboratory Medicine*. **2008**, *46*, 1589–1597.

[33] M. Golovko, E. Murphy. An improved LC-MS/MS procedure for brain prostanoid analysis using brain fixation with head-focused micro wave irradiation and liquid-liquid extraction. *Journal of Lipids.* **2008**, *49*, 893–902.

[34] T.M. Miller, M.K. Donnelly, E.A. Crago, D.M. Roman, P.R. Sherwood, M.B. Horowitz, S.M. Poloyac. Rapid, simultaneous quantitation of mono and dioxygenated metabolites of arachidonic acid in human CSF and rat brain. *Journal Chromatography. B*, **2009**, *877*, 3991–4000.

[35] Y. Tajima, M. Ishikawa, K. Maekawa, M. Murayama, Y. Senoo, T. Nishimaki-Mogami, H. Nakanishi, K. Ikeda, M. Arita, R. Taguchi. Lipidomic analysis of brain tissues and plasma in a mouse model expressing mutated human amyloid precursor protein/tau for Alzheimer's disease. *Lipids in Health and Disease*. ***2013***, *12*, 68.

[36] H. Liu, W. Li, M. Ahmad, M.E. Rose, T.M. Miller, M. Yu, J. Chen, J.L. Pascoe, S.M. Poloyac, R.W. Hickey. Increased Generation of Cyclopentenone Prostaglandins after brain ischemia and their role in aggregation of ubiquitinated proteins in neurons neurotoxicology. **2013**, *24*, 191–204.

[37] S. Meydani, A. Shapiro, M. Meydani, J. Blumberg: Lung eicosanoid synthesis is affected by age, dietary fat and vitamin E. *The Journal of Nutrition*. **1992**, *122*, 1627-1633.

[38] J.Y. Westcott, S. Chang, M. Balazy, D.O. Stene, P. Pradelles s, J. Maclouf, N.F. Voelkel, and R.C. Murphy. Analysis of 6-Keto PGFI~, 5-HETE, and LTC4 in rat lung: Comparison of GC/MS, RIA. and EIA. *Prostaglandins.* **1986**, *32*, 857-873.

[39] C. Margaret. C. Schmidt, S. Faicloth, J. Weete. Modulation of avian lung eicosanoids by dietary omega-3 fatty acids. *Journal of Nutrition*. **1987**, *117*, 1197-1206.

[40] H. I Jsselstijn, F. J. Zijlstra, J. P. M. van Dijk, J. C. de Jongste and D. Tibboel. Lung eicosanoids in perinatal rats with congenital diaphragmatic hernia. *Mediators of Inflammation*, **1997**, *6*, 39-45.

[41] F. Campbell, P. Chanez, C. Marty-Ané, B. Albat, Bloom, Michel FB, Godard P, J. Bousquet. Modulation of eicosanoid and histamine release from human dispersed lung cells by terfenadine. *Allergy*. **1993**, *48*, 125-129.

[42] N.Ohara, N.Voekel and S.Chang. Tissue eicosanoids and vascular permeability in Rats with chronic biliary obstruction. *Hepatology*. **1993**, *18*, 111-118.

[43] D. Cha, M. Liu, Z. Zeng, D. Cheng, G. Zhan. Analysis of fatty acids in lung tissues using gas chromatography-mass spectrometry preceded by derivatization solid phase micro extraction with a novel fiber. *Analytical Chemistry Acta***. 2006**, *572*, 47–54.

[44] K. Sagliani, S. Hill, B. Fanburg, G. Dolnikowski, B. Levy, I. Preston. LC/MS/MS method for simultaneous analysis of arachidonic acid and its endogenous eicosanoid metabolites and prostaglandins in rodent lung tissue. *Pulmonary Circulation*. **2013**, *3*, 82–88.

[45] D. Sagliani, G Dolnikowski, N. Hill, B. Fanburg, B. Levy, I Preston. LC/MS/MS method for simultaneous analysis of arachidonic acid and its endogenous eicosanoid metabolites and prostaglandins in rodent lung tissue. *Experimental Models In Pulmonary hypertension.* **2012**, A3428

[46] N. Degousee, D. Kelvin, G. Geisslinger, D. Hwang. Group V phospholipase A_2 in bone marrow-derived myeloid cells and bronchial epithelial cells promotes bacterial clearance after Escherichia coli pneumonia. *Journal of Biology and Chemistry*. **2011**, *41*, 35650–35662.

[47] L. Kiss & Y. Röder and J. Bier. Direct eicosanoid profiling of the hypoxic lung by comprehensive analysis via capillary liquid chromatography with dual online photodiode-array and tandem mass-spectrometric detection. *Analytical Bioanalysis Chemistry*. **2008**, *390*, 697–714.

[48] H. Hanaka, S. Pawelzikb, j. Johnsen, M. Rakonjaca, K. Terawakia, A. Rasmusonc, Microsomal prostaglandin E synthase 1 determines tumor growth in vivo of prostate and lung cancer cells. *PNAS*. **2009**, *44*, 18757–18762.

[49] V. E. Kelley, S. Sneve, and S. Musinski. Increased Renal Thromboxane Production in Murine Lupus Nephritis. *Journal of Clinical Investigation*. **1986**, *77*, 252-259.

[50] G Rae, M. Trybulec, G. de Nucci and J. Vane. Endothelin-1 releases eicosanoids from rabbit isolated perfused kidney and spleen. *Journal of Cardiology and Pharmacy*. **1989**, *13,* 89-92.

[51] A.J. Blewett, D. Varma, T. Gilles, J. R. Libonati. Development and validation of a high-performance liquid chromatography electrospray mass spectrometry method for the simultaneous determination of 23 eicosanoids S. A. Jansen. *Journal of Pharmacy and Biology Analysis*. **2006**, *46*, 653–662.

[52] S. A. Brose and M. Y. Golovko. Eicosanoid post-mortem induction in kidney tissue is prevented by microwave irradiation. *Prostaglandins, Leukotrienes and Essential Fatty Acids*. **2013,** *89*, 313–318.

[53] Y. Wanga, A. M. Armandob, O. Quehenbergerb, C. Yana, E. A. Dennis. Comprehensive ultra-performance liquid chromatographic separation and mass spectrometric analysis of eicosanoid metabolites in human samples. *Journal of Chromatography A*. **2014**, *1359*, 60–69.

[54] V. Blaho, M. Buczynski, C. R. Brown, and E. A. Dennis. Lipidomic analysis of dynamic eicosanoid responses during the induction and resolution of Lyme arthritis. *Journal of biological chemistry*. **2009**, *284*, 21599–21612.

[55] D. Aked and S. Foster. Leukotriene B4 and prostaglandin E2 mediate the inflammatory response of rabbit skin to intradermal arachidonic acid. *British Journal of Pharmacology*. **1987**, *92*, 545-552.

[56] D. M. Reilly and M. R. Green. Eicosanoid and Cytokine Levels in Acute Skin Irritation in Response to Tape Stripping and Capsaicin. *Acta Dermato-Venereologica.* **1999**, *79*, 187-190.

[57] J. Ghioni. Bell, M. V. Bell and J. R. Sargent. Fatty acid composition, eicosanoid production and permeability in skin tissues of rainbow trout (Oncorhynchusmykiss) fed a control or an essential fatty acid deficient diet. *Prostaglandins, Leukotrienes and Essential Fatty Acids*. **1997**, *56*, 479-489.

[58] L. E. Rhodes, K. Gledhill, M. Masoodi, A. K. Haylett. The sunburn response in human skin is characterized by sequential eicosanoid profiles that may mediate its early and late phases. *FASEB Journal*. **2009**, *23*, 3947–3956.

[59] Ferretti, V. Flangan, and J. Roman. Quantitative measurement of prostaglandins E 2 and E 3 by selected ion monitoring. *Lipids.* **1982**, *17*, 825-830.

[60] S. Ödergen. Lipid peroxidation in vivo evaluation and application of methods for measurement. Comprehensive summaries of Uppsala dissertations from the faculty of medicine, **2011**, *Uppsala*. ISBN 91-554-4791-0.

[61] R. Peebles, H. Glauert. Effect of phenobarbital on hepatic eicosanoid concentrations in rats. *Archive Toxicology*. **1997**, *71*, 646-650.

[62] J. Gonzalez, A. Planaguma, K. Gronert, R. Miquel. Docosahexaenoic acid (DHA) blunts liver injury by conversion to protective lipid mediators: protectin D1 and 17S-hydroxy-DHA. *FASEB Journal*. **2006**, *20*, E000–E000

[63] M. Balvers, K. Verhoeckx , J. Meijerink , S. Bijlsma. Time-dependent effect of in vivo inflammation on eicosanoid and endocannabinoid levels in plasma, liver, ileum and adipose tissue in C57BL/6 mice fed a fish-oil diet. *International Immunopharmacology*. **2012**, *13*: 204–214.

[64] T. Koal, G.K. Weinberger, K.M. Ramsay; Rapid sample preparation and simultaneous quantitation of prostaglandins and lipoxygenase derived fatty acid metabolites by liquid chromatography-mass spectrometry from small sample volumes. *Clinical Chemistry and Laboratory Medicine*. **2008**, *46*, 1589-1597.

[65] M. Coffa and E. M. Hill. Discovery of an 11(R)- and 12(S)-Lipoxygenase activity in ovaries of the mussel Mytilusedulis. *Lipids.* **2000**, *35*, 1195–1204.

[66] R. S. Freedman, E. Wang, S. Voiculescu, R. Patenia, R. L. Bassett. Comparative Analysis of Peritoneum and Tumor Eicosanoids and Pathways in Advanced Ovarian Cancer. *Clinical Cancer research*. **2007**, *13*, 19-27.

[67] S. Janagap, R. Azeredo, T. Nguyen, K. Hamre, P. Araujo. Development of an extraction method for the determination of prostaglandins in biological tissue samples using liquid chromatography–tandem mass spectrometry: Application to gonads of Atlantic cod (Gadusmorhua). *Analytica Chimica Acta*. **2012**, *749*, 51– 55.

[68] M. F. Mc Entee, C. Ziegler, D. Reel, K. Tomer, A. Shoieb, M. Ray, X. Li. Dietary n-3 polyunsaturated fatty acids enhance hormone ablation therapy in Androgen-Dependent Prostate Cancer. *American Journal of Pathology*. **2008**, *173*, 229–241.

[69] W. Kort, A. Bijma, J. van Dam, A. van der Ham, J. Hekking, H. van der Ingh. Eicosanoids in breast cancer patients before and after mastectomy. *Prostaglandins Leukotrienes Essential Fatty Acids***. 1992**, *45*, 319–327.

[70] N.K. Boughton-Smith, J.L. Wallace, G.P. Morris and B.J.R. Whittle. The effect of anti-inflammatory drugs on eicosanoid formation in a chronic model of inflammatory bowel disease in the rat. *British Journal Pharmacology*. **1988**, *94*, 65-72.

[71] N. Boughton-Smith, L. Wallace and M. Whittle. The effect of anti-inflammatory drugs on eicosanoid formation in a chronic model of inflammatory bowel disease in the rat. *British Journal of Pharmacology*. **1988**, *94*, 65-72.

[72] C. J. Bell, E. J. Elliott, J. L. Wallace, D. M. Redmond, J. Payne, Z. Li and E. V. O'Loughlin. Do eicosanoids cause colonic dysfunction in experimental *E coli* 0157:H7 (EHEC) infection? *Journal of the Gut*. **2000**, *46*, 806–812

[73] J. W. Bregano, D. S. Barbosa, M. Z. Kadri, M. A. Rodreges. Comparison of selective and non selective cyclo-oxygenase 2 Inhibitor in experimental colitis exacerbation: role of leukotriene B4 and superoxide dismutase. *Archivos Gastroenterologia*. **2014**, *51*, 226-234.

[74] N. Nieto, M.I. Fernandez, M.I. Torres, A. Raios, M.D. Suarez, and A. Gil. Dietary monounsaturated n-3 and n-6 long-chain polyunsaturated fatty acids affect cellular

antioxidant defense system in rats with experimental ulcerative colitis induced by trinitrobenzene sulfonic acid. *Digestive Diseases and Sciences*. **1998**, *43*, 2676-2687.

[75] T. Moses, L. Wagner and S.D. Fleming. TLR4-mediated Cox-2 expression increases intestinal ischemia/reperfusion-induced damage. *Journal of leukocyte biology*. **2009**, *86*, 971–980.

[76] N. Bosco, V. Brahmbhatt, M. Oliveira, F. Martin, P. Lichti, F. Raymond, Effects of increase in fish oil intake on intestinal eicosanoids and inflammation in a mouse model of colitis. *Lipids in Health and Disease*. **2013**, *12*, 81-90.

[77] S.M. Zick, D. K, Turgeon and S.K. Vareed. Eicosanoids in colon mucosa in people at normal risk for phase II study of the effects of ginger root extract on colorectal cancer. *Cancer Preventive Research*. **2011**, *4*, 1–9

[78] M. Masoodi, D. Pearl, M Eiden, J. Shute, J. Brown. Altered colonic mucosal polyunsaturated fatty acid (PUFA) derived lipid mediators in ulcerative colitis: New insight into relationship with disease activity and pathophysiology. *Plos one.* **2013**, *10*, e76532.

[79] V. Dijk, J. Wilsona and F. Zijlstra. The effect of malotilate, a derivative of rnalotilate and a flavonoid on eicosanoid production in inflammatory bowel disease in rats. *Mediators of Inflammation*. **1993**, *2*, 67-72.

[80] Y. Fan, J. M. Monk, T. Hou, E. Callway, L. Vincent. Characterization of an arachidonic acid-deficient (Fads1 knockout) mouse model. *Journal of Lipid Research.* **2012**, *53*, 1287–1295.

[81] M. Mal, P. Koh, P. Cheah, E. Chan. Ultra-pressure liquid chromatography/tandem mass spectrometry targeted profiling of arachidonic acid and eicosanoids in human colorectal cancer. *Rapid communication in mass spectroscopy*. **2011**, *25*, 755-764.

[82] Z. Mangesha. Development of an extraction method for the analysis of pro-inflammatory prostaglandin-E2 and leukotriene-B4 in human plasma by liquid chromatography tandem mass spectrometry. *Master Thesis, UiB publication*. **2013**.

[83] P. Araujo, Z. Mangesha, E. Lucena and B. Grung. Development and validation of an extraction method for pro-inflammatory eicosanoids in human plasma using liquid chromatography tandem mass spectrometry. *Journal of chromatography A*. **2014**, *1353*, 57-64.

[84] L. Eriksson, E. Johansson, C. Wikstrom. Mixture design—design generation, PLS analysis, and model usage. *Chemometrics and Intelligent Laboratory Systems*. **1998,** *43*, 1–24.

[85] P. Araujo, F. Couillard, E. Leirnes, K. Ask, A. Bøkevoll, L. Frøyland. Experimental design considerations in quantification experiments by using the internal standard technique: Cholesterol determination by gas chromatography as a case study. *Journal of Chromatography A*. **2006**, *1121*, 99–105.

[86] W. Huber, A. Molero, C. Pereyra, E. Martfnez de la Ossa. Determination of cholesterol in milk fat by supercritical fluid chromatography. *Journal of Chromatography A*. **1995**, *715*, 333-336.

[87] D.J. Fletouris N.A. Botsoglou, I.E. Psomas, A.I. Mantis. Rapid determination of cholesterol in milk and milk products by direct saponification and capillary gas chromatography. *Journal of Dairy Science*. **1998**, *81*2, 833–2840.

[88] D.H. Doehlert. Uniform shell design. *Application of Statistic*. **1970**, *19*, 231.

[89] P. Araujo, R. G. Brereton. Visualisation of confidence in Two-factor designs where model, replication and star points are varied. *Analyst*. **1997**, *122* (621–630).

[90] J. Bell, J. Castell, D. Tocher, F. MacDonald, J. Sargent. Effects of different dietary arachidonicacid:docosahexaenoic acid ratios on phospholipid fatty acid compositions and prostaglandin production in juvenile turbot (Scophthalmusmaximus). *Fish Physiology and Biochemistry*. **1995**, *14*, 139-151.

[91] J. Bell, D. Tocher, B. Farndale, D. Cox, W. McKinneyc, J. Sargent. Modification of membrane fatty acid composition, eicosanoid production, and phospholipase A activity in Atlantic Salmon (Salmosalar) gill and kidney by dietary lipid. *Lipids*. **1997**, *32*, 515–525.

[92] J. Miller. Statistics and chemometrics for analytical chemistry. 6th edition. **2010**, 127-131.

[93] L. Rodrıguez, M. Gonzalez, M. Vinas, A. Casado, A. Gomez Principles of analytical calibration/quantification for the separation sciences. *Journal of Chromatography A*. **2007**, *1158*, 33–46.

[94] K. Tolman. Eicosanoids and the liver. *Prostaglandins & other Lipid Mediators*. **2000**, *61*, 163–174.

[95] P. Araujo. Key aspects of analytical method validation and linearity evaluation. *Journal of Chromatography B*. **2009**, *877*, 2224–2234.

[96] R. Ardrey. Liquid Chromatography– Mass Spectrometry: An Introduction. **2003,** 7-31.

[97] D. Tiskas. A proposal for comparing methods of quantitative analysis of endogenous compounds in biological systems by using the relative lower limit of quantification (rLLOQ). *Journal of Chromatography B*. **2009**, *877*, 2244–2251.

[98] E. Rozet, A. Ceccato, C. Hubert, E. Ziemons, S. Rudaz, B. Boulanger, P. Hubert . Analysis of recent pharmaceutical regulatory documents on analytical method validation. *Journal of Chromatography A*, **2007**, *1158*, 111–125.

[99] Hill A. Reynolds S. Guidelines for in-house validation of analytical methods for pesticide residues in food and animal feeds. The Analyst perspective, **1999**, *124*, 953–958.

[100] H. Cao, L. Xiao, G. Park, X. Wang, A. Azim, J. Christman, and R. van Breemen. An improved LC-MS-MS method for the quantification of prostaglandins E2 and D2 production in biological fluids. *Analytical Biochemistry*, **2008**, *372*, 41–51.

[101] E. Blich, W. Dyer. A rapid method for total lipid extraction and purification. **1959,** *37*, 911-917.

Appendix 1. The Weight of samples used in Doelhert design experiments and the corresponding analyte and internal standard both real and theoretical concentration

Sample number	Weight (g)	Corresponding experimental point in the Doelhert design	Theoretical concentration ng/g		Analyte real concentration ng/g	
			[A]	[IS]	[A]	[IS]
1	0.35	1	25.00	32.50	21.38	27.79
2	0.28	1	25.00	32.50	26.28	34.19
3	0.29	1	25.00	32.50	26.20	34.07
4	0.33	2	13.20	17.30	33.52	15.57
5	0.27	2	13.20	17.30	41.73	19.38
6	0.30	3	50.00	47.70	13.40	48.43
7	0.36	3	50.00	47.70	11.11	40.14
8	0.35	4	13.20	17.30	11.18	14.65
9	0.35	4	13.20	17.30	11.20	14.69
10	0.28	4	13.20	17.30	14.17	18.58
11	0.27	5	37.25	47.70	41.01	52.51
12	0.29	5	37.25	47.70	38.64	49.48
13	0.27	5	37.25	47.70	41.50	53.14
14	0.34	6	1.00	32.50	0.87	28.39
15	0.28	6	1.00	32.50	1.06	34.57
16	0.29	7	50.00	32.50	51.44	33.44
17	0.32	7	50.00	32.50	47.47	30.85
18	0.30	8	0	17.30	0	16.91
19	0.35	9	0	32.50	0	28.05
20	0.33	9	0	32.50	0	29.58
21	0.29	10	0	47.70	0	49.60